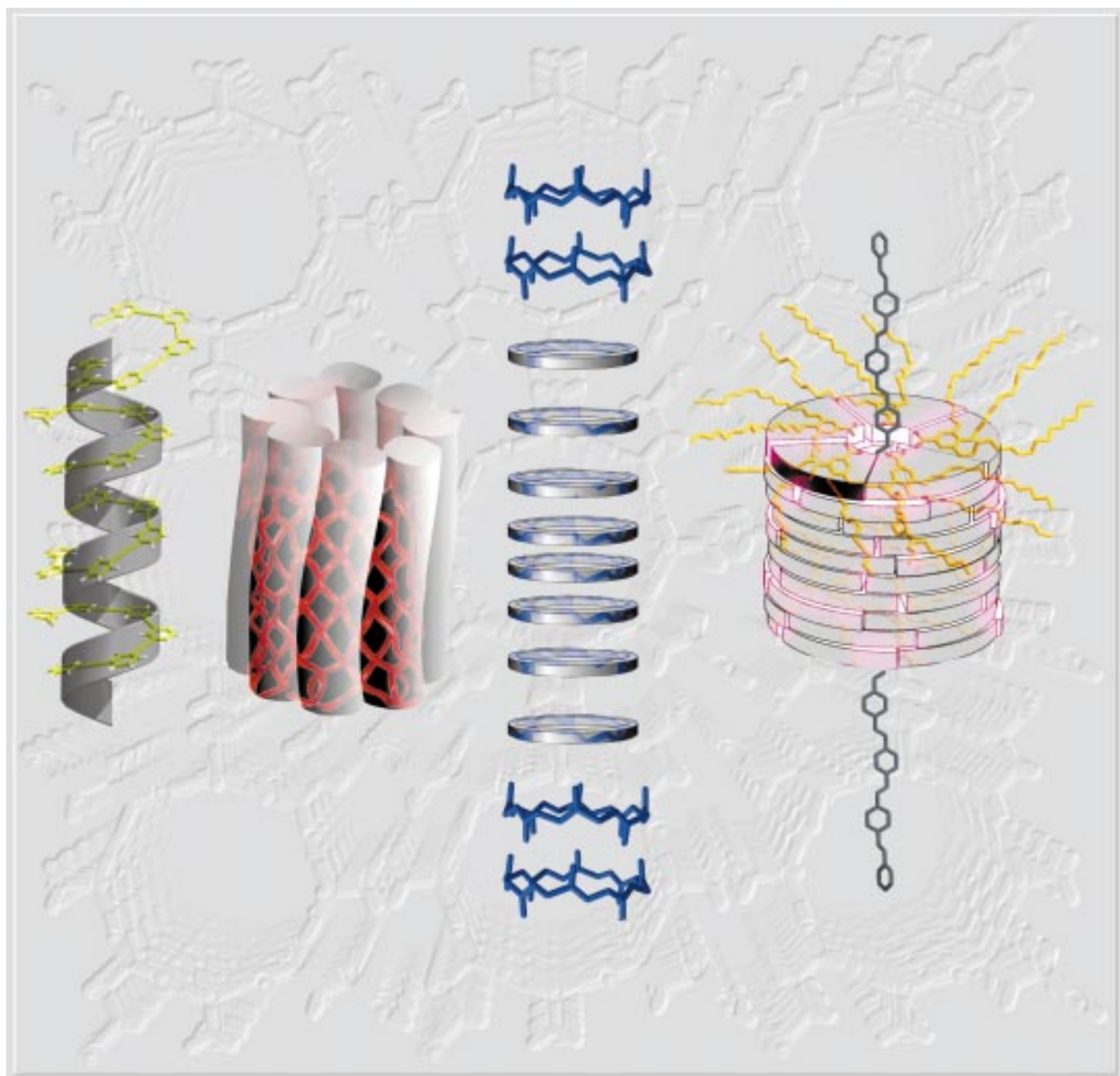


Organic Nanotubes



Self-Assembling Organic Nanotubes

Dennis T. Bong, Thomas D. Clark, Juan R. Granja, and M. Reza Ghadiri*

Hollow tubular structures of molecular dimensions perform diverse biological functions in nature. Examples include scaffolding and packaging roles played by cytoskeletal microtubules and viral coat proteins, respectively, as well as the chemical transport and screening activities of membrane channels. In the preparation of such tubular assemblies,

biological systems make extensive use of self-assembling and self-organizing strategies. Owing to numerous potential applications in areas such as chemistry, biology, and materials science considerable effort has recently been devoted to preparation of artificial nanotubular structures. This article reviews design principles and the prepa-

ration of synthetic organic nanotubes, with special emphasis on noncovalent processes such as self-assembly and self-organization.

Keywords: crystal engineering • materials science • nanotubes • self-assembly • sensors

1. Introduction

Organic tubular assemblies are of interest due to their numerous possible applications, many of which are evident from a consideration of biological systems. For example, hollow tubular structures act as conduits of chemical information in the form of transmembrane ion channels^[1] and provide closed reaction chambers, as demonstrated by protein-folding chaperonins^[2, 3] and protein-degradation enzymes.^[4, 5] The cylindrical internal surfaces of these protein compartments are well suited for the presentation of chemical functionality, thus enhancing enzyme activity through functional-group complementarity and chemical catalysis. Furthermore, the bounded nature of the cylinder allows selectivity on the basis of substrate size. The membrane protein aquaporin provides a striking demonstration, as it transports

only water through its central pore and discriminates against all other small polar molecules.^[6]

Inspired by the remarkable functions of tubular structures in biology, much research has focussed on the construction of simpler synthetic tubes for application as specific ion sensors, easily tailored molecular reaction vessels, molecular sieves, or nanoscale fluidic transport systems. An equally intense effort has aimed to apply biologically derived design principles to the construction of functional tubular materials with no known biological analogue. Examples include liquid crystal display components and birefringent materials. While many advances have been reported regarding porous inorganic materials and carbon nanotubes, this review will center on the contributions made by synthetic and bioorganic chemistry to the preparation of tubular constructs. Special attention will be given to noncovalent processes as these strategies possess several inherent advantages over covalent syntheses, the most noteworthy of which include high synthetic convergence, built-in error-correction, control of assembly through subunit design, and overall high efficiency.^[7, 8]

2. Motifs of Tubular Assembly

Conceptually, there are several possible ways to design open-ended hollow tubular structures (Figure 1). For example, a two-dimensional sheet-like starting material can be either rolled or sealed at opposing edges to yield a tube-shaped construct. Such processes have been noted in formation of carbon nanotubes from graphite.^[9, 10] Emulsion-templated mineralization or polymerization is another approach which has proven to be of exceptional utility in the

[*] Prof. Dr. M. R. Ghadiri, D. T. Bong, Dr. T. D. Clark,
Prof. Dr. J. R. Granja
Departments of Chemistry and Molecular Biology
and the Skaggs Institute for Chemical Biology
The Scripps Research Institute
10550 North Torrey Pines Road, La Jolla, CA 92037 (USA)
Fax: (+1) 858-784-2798
E-mail: ghadiri@scripps.edu
Dr. T. D. Clark
Department of Chemistry and Chemical Biology
Harvard University
12 Oxford Street, Cambridge, MA 02138 (USA)
Prof. Dr. J. R. Granja
Departamento de Química Orgánica
Facultad de Química
Universidad de Santiago de Compostela
15706 Santiago de Compostela (Spain)

preparation of porous silicates and related mesoporous materials.^[11–14] Hollow structures can also be formed by assembly of stave or rod-like subunits into barrel or bundle-shaped frameworks. Examples of this motif include trans-membrane pores formed by β -barrel proteins such as α -hemolysin^[15] and porins,^[16–18] as well as α -helical bundles of cholera toxin^[19] and the potassium channel.^[20] Linear precursors can form tubular structures by coiling into hollow, helical conformations. This motif is illustrated by β -helical structures formed by the natural antibiotic gramicidin A.^[21]

Finally, tubular arrays can be prepared from the stacking of disc or sector-shaped subunits. Self-assembly of the tobacco mosaic virus (TMV) coat protein is perhaps the best known biological instance of this motif.^[22, 24, 25] Of these various approaches, the last three have thus far offered the most design flexibility and synthetic convergence. As detailed in the following sections, most approaches towards tubular constructs have been biomimetic; in general, the self-assembly strategies have resonance with those found in biological systems.



D. T. Bong



T. D. Clark



J. R. Granja



M. R. Ghadiri

Dennis T. Bong was born in Victoria, Canada, in 1974. He received his BSc in chemistry from the University of California, Berkeley, in 1994. During his stay at Berkeley, he also received his initiation in chemical research under the guidance of Professor K. Peter C. Vollhardt, studying the physical organic chemistry of strained aromatic systems. From Berkeley he moved to La Jolla, California, to join the chemistry graduate program at the Scripps Research Institute where he is currently completing his PhD work in membrane biophysics, supramolecular chemistry, and de novo protein design under the direction of Professor M. Reza Ghadiri. Research interests in bioorganic chemistry have prompted him to take up a postdoctoral position in the laboratory of Professor Ronald Breslow at Columbia University in New York following the closure of his PhD studies.

Thomas D. Clark was born in Burlington, Vermont, in 1970 and received his BA in chemistry from Boston University. As an undergraduate he studied synthetic organic chemistry in the laboratory of Professor James Panek. In 1998 he received his PhD in chemistry from The Scripps Research Institute, where he worked with Professor M. Reza Ghadiri on the design and characterization of self-assembling cyclic peptide nanotubes. He is currently investigating new methods of microfabrication based on self-assembly of micron-sized objects in the laboratory of Professor George Whitesides at Harvard University. His other research interests include the preparation of functional biomaterials for diagnostic and research applications.

Juan R. Granja was born in Villagarcia de Arosa, Spain, in 1961 and received his PhD in chemistry in 1988 from the University of Santiago de Compostela under the supervision of Professors A. Mourino and L. Castedo. After a two-year postdoctoral stint in the group of Professor Barry M. Trost at Stanford University, he obtained a position as Assistant Professor at the University of Santiago, and was promoted to Associate Professor in 1995. In 1993, he spent six months as visiting scholar in the group of Professor M. Reza Ghadiri at the Scripps Research Institute, working on the design and synthesis of peptide nanotubes. Since then, he has been collaborating with the Ghadiri group on the design, synthesis, and applications of peptide nanotubes and on the development of new catalytic and self-replicating processes using small peptides. His research interests are presently focused on the design and synthesis of artificial self-assembling peptide systems and new approaches for the synthesis of polycarbocycle systems of biological interest.

M. Reza Ghadiri was born in Tehran, Iran, in December 1959. He received his bachelor degree from the University of Wisconsin, Milwaukee, in 1982 and his PhD in synthetic organic chemistry from the University of Wisconsin, Madison, in 1987, under the guidance of Professor Barry M. Trost. After a two-year postdoctoral fellowship studying enzymology and molecular biology in the laboratory of the late Professor Emil T. Kaiser at the Rockefeller University, he joined the Faculty of Chemistry at the Scripps Research Institute. He is presently Professor of Chemistry and Molecular Biology, and a member of the Skaggs Institute for Chemical Biology. His current research interests include design of functional peptide assemblies, catalyst engineering, molecular logic gates, nonlinear chemical networks and ecosystems, novel biomaterials and composites, and proteomics.

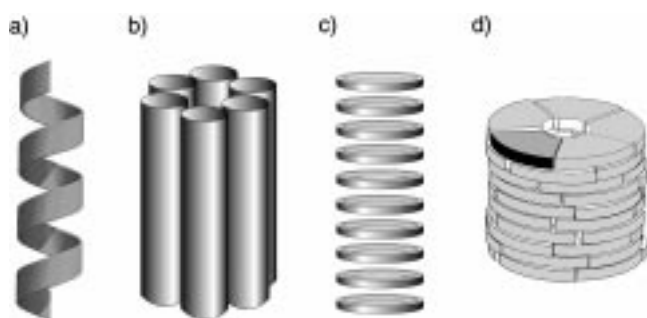


Figure 1. Four possible strategies for the molecular assembly of tubular materials. a) Helical molecules can be coiled to form hollow, folded structures, b) rod-like molecules can be assembled in a barrel-stave fashion to form molecular bundles, c) macrocycles can be stacked to form continuous tubes, and d) sector or wedge-shaped molecules can assemble into discs that subsequently stack to form continuous cylinders, similar to macrocycles.

3. Hollow Coiled Molecules

3.1. Linear D,L-Peptides Form Cylindrical β - or π_{DL} -Helices

The β - or π_{DL} -helices are peptide supersecondary structural motifs in which the backbone folds into a helical conformation stabilized by β -sheet-type hydrogen bonding. First proposed in 1971 by Urry and independently by Ramachandran and Chandrasekaran in 1972, β -helical conformations are common in linear peptides composed of alternating D- and L- α -amino acids (D,L-peptides) due to the conformational requirements for β -sheet hydrogen bonding.^[26, 27] As noted initially by Pauling and Corey, residues in extended sheets must assume pleated conformations in order to alleviate side chain to side chain steric clashes that would result if the residues adopted a fully extended conformation.^[28] For an idealized β -strand composed of all L-amino acids ($C\alpha-N$ torsion angle $\phi_L = -120^\circ$, $C\alpha-C$ torsion angle $\psi_L = 120^\circ$), the pleating of adjacent residues causes the direction of the peptide backbone to alternate in sinusoidal fashion (Figure 2a). Inverting the chirality (L \rightarrow D) of a single residue while maintaining a pleated conformation also requires inverting its backbone dihedral angles ($\phi_D = 120^\circ$, $\psi_D = -120^\circ$), since equivalent conformations of L- and D-residues are related by a factor of -1 .^[27, 29] The direction of pleating in the D-residue reinforces that of the adjacent L-residues and gives rise to an overall bend; inverting the chirality and dihedral angles of every second residue causes the backbone to bend continuously (Figure 2b, c). The peptide can now conveniently satisfy its hydrogen-bonding requirements by adopting a helical conformation (Figure 2d) with quasi-equivalent conformations of L- and D-residues ($\phi_L = -133^\circ$, $\psi_L = 117^\circ$; $\phi_D = 118^\circ$, $\psi_D = -130^\circ$).^[29] Such an idealized β -helix displays screw axis symmetry with a repeat unit of two residues.

While monomeric β -helices necessarily exhibit parallel β -sheet hydrogen bonding, entwined double-stranded parallel ($\uparrow\uparrow$) and antiparallel ($\uparrow\downarrow$) helices are also possible.^[30] β -helices can exist in either right- or left-handed conformations depending on peptide length, residue composition, and prevailing chirality.^[27, 30] In all such structures, amino acid

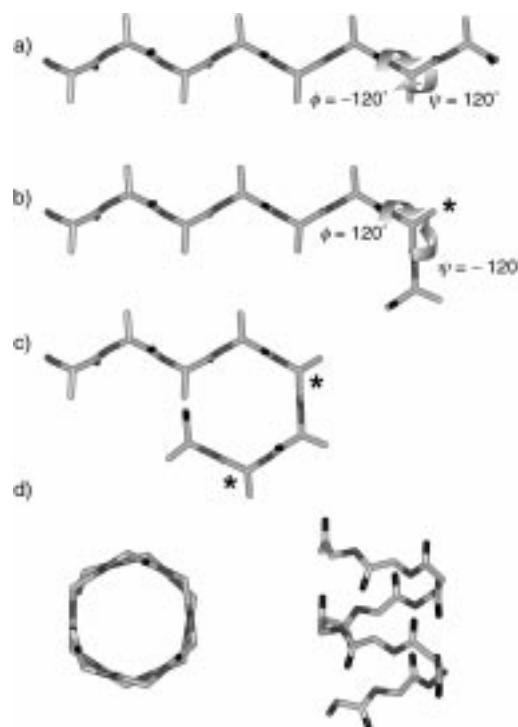


Figure 2. The relationship between the conformation of a β -pleated strand and that of a β -helix. a) An all-L peptide in an idealized pleated β -conformation ($\phi = -120^\circ$, $\psi = 120^\circ$) viewed parallel to the plane of the backbone amide groups (for clarity only the backbone and C_β atoms are shown). b) The chirality of the residue marked with an asterisk has been inverted from L to D. In order to maintain a pleated conformation capable of participating in β -type hydrogen bonding, the backbone dihedral angles of this residue must also be inverted ($\phi = 120^\circ$, $\psi = -120^\circ$). This causes a kink in the peptide chain. c) Inversion of the chirality and backbone dihedral angles of another residue one removed from the first gives rise to a loop in the peptide chain. d) Performing these operations on every second residue causes the peptide chain to bend continuously and form a β -helix. On the left, the β -helix is viewed parallel to the helix axis, emphasizing its internal pore 3.3 Å in diameter. On the right the β -helix is viewed perpendicular to its helical axis in order to illustrate its intrachain β -type hydrogen-bonding pattern. For clarity only the backbone atoms are shown.

side chains radiate outward, leaving an unoccluded central pore running the length of the helix axis. The average radius of the β -helix pore depends upon the helix periodicity, or number of residues per turn (expressed as a superscript; for example, $\beta^{5.6}$ signifies a β -helix with 5.6 residues per turn), with larger periodicities giving rise to larger pores. In principle, helix periodicity can be controlled by varying the backbone hydrogen-bonding register, making β -helices potentially attractive scaffolds for preparation of tubular structures with tailored internal dimensions.^[27, 29] Indeed, computational studies have indicated that single-stranded β -helices with 4.8, 6.2, and 8.2 residues per turn should display pore diameters of 2.3, 3.3, and 4.7 Å, respectively.^[29]

Interest in β -helical structures can be traced to a 1941 report describing isolation and partial characterization of a mixture of *Bacillus brevis* peptide antibiotics known collectively as gramicidin.^[31] Degradation studies revealed that the major constituent, named gramicidin A, is a linear penta-decapeptide composed of alternating D- and L-amino acids with the following primary structure: HCO-L-Val-Gly-L-Ala-

D-Leu-L-Ala-D-Val-L-Val-D-Val-L-Trp-D-Leu-L-Trp-D-Leu-L-Trp-NHCH₂CH₂OH.^[32–35] Recognition of the transmembrane pore-forming ability of gramicidin A^[36] led to a number of proposed models for the active species. Based on conformational analysis, in 1971 Urry put forth a structure in which the molecule adopts β -sheet-type torsion angles, with the alternating chirality of adjacent residues giving rise to helical curvature reinforced by interresidue hydrogen bonding.^[26] The dependence of equilibrium conductance on antibiotic concentration,^[37] coupled with the requirement that the active form of gramicidin A be of sufficient length to span a lipid bilayer wider than 35 Å, prompted Urry to suggest a dimeric structure in which two single β -helices associate in a head-to-head fashion through backbone–backbone hydrogen bonding.^[26] Recent solid-state NMR spectroscopy work in a lipid medium has confirmed the essential features of this model.^[21]

Early studies of synthetic β -helices focused on syndiotactic homopolydipeptides.^[38, 39] In particular, X-ray and electron fiber diffraction studies of poly- γ -benzyl-D,L-glutamate demonstrated that the polymer can exist in not only single- but also double-stranded β -helical conformations.^[40, 41] While double- or higher stranded helical structures had long been known for polynucleotides and certain polysaccharides, these were the first such structures documented for polypeptides. The periodicity of β -helices obtained in crystalline samples ranged from 5.6 to 10.9 residues per turn and was found to be highly dependent on the crystallization solvent. These observations were rationalized in terms of expansion or contraction of the helical pore to accommodate included solvent molecules.^[41]

In 1975 DeSantis and co-workers reported the first attempts at preparing β -helix-forming oligopeptides of discrete length.^[39] In the solid state, peptides of general sequence X(L-Ala-D-Val)_{*m*}Y displayed X-ray powder diffraction patterns consistent with α -pleated structures^[28, 29, 42] while circular dichroism (CD) spectra of the polymer in trifluoroethanol (TFE) suggested a β -helical conformation. In addition, ¹H NMR spectra ([D₆]DMSO) of hexa- and octapeptides (X = benzyloxycarbonyl (Cbz), Y = OMe) were well dispersed and showed ³J_{NH,αH} values of nearly 8.5 Hz, which strongly evince β -type ϕ torsion angles.

In 1979 an X-ray crystallographic study of octapeptide Boc-(L-Val-D-Val)₄-OMe (Boc = *tert*-butoxycarbonyl) by Lorenzi and co-workers provided the first atomic resolution structure of a β -helical peptide.^[43, 44] The compound crystallized as a C₂-symmetrical left-handed double $\beta^{5,6}$ -helix. Later NMR studies supported the existence of similar left-handed double helical structures in solution.^[45–47] Related higher homologues were found to exist predominantly as a mixture of monomeric left- and right-handed $\beta^{4,4}$ -helices, presumably due to an increased opportunity for intramolecular hydrogen bonding as compared with the octapeptide.^[48–50] Lorenzi and co-workers also observed gramicidin-like head-to-head dimerization of monomeric $\beta^{4,4}$ -helices formed by *N*-formylated nonapeptide HCO-L-Ile-(D-allo-L-Ile)₄-OMe^[51] (allo = allo-isoleucine), as well as tetramerization of heptapeptide HCO-L-Phe-(D-Phe-L-Phe)₄-OMe to give an unusual head-to-head dimer of double-stranded $\uparrow\uparrow\beta^{5,6}$ -helices.^[52]

Mirroring the findings with other β -sheet model systems,^[53–55] Lorenzi and co-workers indicated that linear stereocooligopeptides (that is, peptides of alternating D,L-configuration) containing β - or γ -branched side chains strongly favor β -helical conformations.^[56] In contrast, the less sterically demanding syndiotactic oligonorleucines between 8 and 15 residues in length did not form β -helices and proved much less soluble in chloroform than related branched species.^[57] The reduced steric bulk presumably results in a lesser degree of β -helical preorganization in the backbone, allowing precipitation through the formation of α -pleated-sheet aggregates.^[28, 29, 42] Introduction of a single backbone *N*-methyl substituent at the (*n* – 3)-position abolished higher order aggregation and led to a mixture of soluble single-stranded $\beta^{4,4}$ - and double-stranded $\uparrow\downarrow\beta^{5,6}$ -helices.^[57] The foregoing studies underscore the strong influence of solvent, peptide length, amino acid composition, and terminating groups on β -helical structures, all of which complicate prediction of the pore size. In addition to a variety of β -helical structures, linear D,L-peptides are also capable of adopting α -helical and α -pleated-sheet conformations.^[58] The conformational promiscuity of these structures, though informative, may undercut their utility in certain applications. It is possible that the membrane-spanning requirement imposed on gramicidin A limits the number of accessible conformations, thus contributing to its reliable formation of the head-to-head dimer in the membrane. Indeed, X-ray crystallographic studies have revealed that gramicidin A can adopt several different conformations in the solid state, depending upon crystallization conditions and the identity of any additives present.^[59–66] However, it is expected that many D,L-peptides of non-gramicidin A sequence would display membrane and possible antibiotic activity,^[67] since membrane insertion should be governed primarily by side-chain hydrophobicity.^[68]

3.2. Helical Folding of Linear Oligophenylacetylenes

Moore, Wolynes, and co-workers have described folding of nonbiopolymers: oligophenylacetylenes can fold into helical conformations.^[69] The design takes advantage of Moore's "shape-persistent" approach to nanoscale architectures in which *n* rigid phenylacetylene subunits are coupled together with a *meta* relationship (Figure 3), and thus nucleate helix-turn conformations within the resulting oligomer.^[70] A helical conformer could be stabilized by solvophobic-driven packing between backbone phenyl rings. Moore reasoned that these interactions would favor self-organization of linear oligomers into folded helical conformations. The relatively wide angle of the turn (approximately 120°) prevents a close-packed core, resulting in a hollow coil reminiscent of peptide β -helices. The spontaneous folding of this linear synthetic polymer into a compact, defined shape places oligophenylacetylenes into the growing family of molecules known as "foldamers".^[71–73]

Linear oligophenylacetylenes with the general structure shown in Figure 3 were studied by UV and NMR spectroscopy. In chloroform solution, Moore and co-workers found

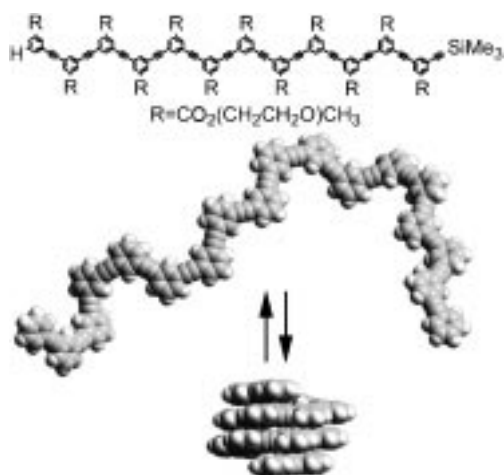


Figure 3. Oligophenylacetylene folding equilibrium between the open state and the helical folded structure (space-filling representation). The ester substituents on each phenyl ring have been omitted in the space-filling model for clarity.^[70] Reprinted with permission from ref. [74]. Copyright (2000) American Chemical Society.

the molar extinction coefficient at 303 nm showed a linear dependence on the length of the molecule. However, in acetonitrile the length dependence was biphasic; compounds with $n > 8$ displayed, per molar phenylacetylene subunit, ϵ_{303} values 35 % smaller than shorter oligomers. This decrease in absorbance was found to be concentration independent, which rules out intermolecular associations, and was attributed to hypochromic effects arising from intramolecular association of aromatic groups. In ^1H NMR spectroscopic experiments, average chemical shifts of aromatic protons were dramatically upfield shifted for $n > 8$, consistent with magnetic shielding due to aromatic π -stacking interactions. The helical nature of these foldamers was assessed by CD studies. As expected, the oligophenylacetylene alone in acetonitrile–water mixtures displays no detectable Cotton effect, since the polymer should exist as a helical racemate. However, when a chiral guest such as α -pinene is added, a clear CD signature is observed in the phenylacetylene absorption region; further, (+)- α -pinene and (–)- α -pinene induce equal and opposite CD spectra (Figure 4).^[74] Binding analyses indicated a 1:1 stoichiometry of association, which suggests binding to the internal hydrophobic pore surface rather than to the outer polar surface. Similar twist-sense bias has been induced in these oligomers by incorporation of a chiral center on the ethylene glycol side chain,^[75] as well as incorporation of an enantiopure binaphthol unit into the phenylacetylene backbone.^[76] Additional support for the formation of a tubular cavity was provided by studies in which a nitrile functionality was incorporated on every other phenyl ring of the dodecamer, *ortho* to both phenylacetylene linkages. This should result in the formation of one trigonal planar metal-binding site per helical turn, which modeling indicated would require six phenylacetylene subunits. Indeed, UV titration studies with AgO_3SCF_3 and electrospray mass spectroscopy revealed a 2:1 stoichiometry of Ag–oligomer binding, to support the notion that helical folding of the oligophenylacetylene occurs with the formation of a tubular cavity which is approximately 4 Å in diameter.^[77]

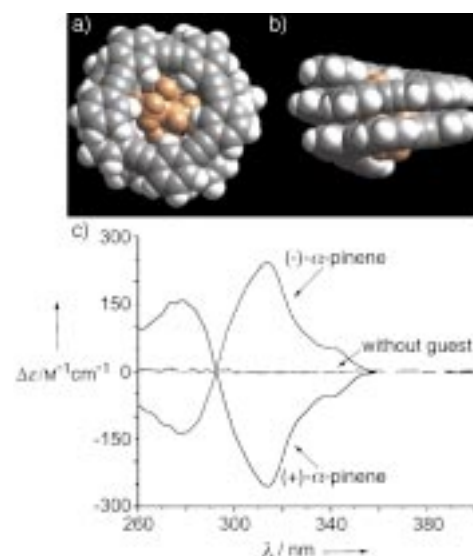


Figure 4. Space-filling model of the oligophenylacetylene shown in Figure 3 coiled around α -pinene: viewed (a) along helical axis and (b) orthogonal to the helical axis.^[74] c) Overlaid CD spectra in acetonitrile/water (60/40). Both the oligophenylacetylene (4.2 μm) and (–)- α -pinene (420 μm) display negligible CD signatures. However, when the two are mixed, a strong positive Cotton effect is observed at 314 nm. The mirror image spectrum is obtained with the oligophenylacetylene and the opposite enantiomer, (+)- α -pinene. Reprinted with permission from ref. [74]. Copyright (2000) American Chemical Society.

Given the facile solid-phase methods for oligophenylacetylene synthesis,^[78] additional interesting derivatives should be readily available to provide further insight into this intriguing system.

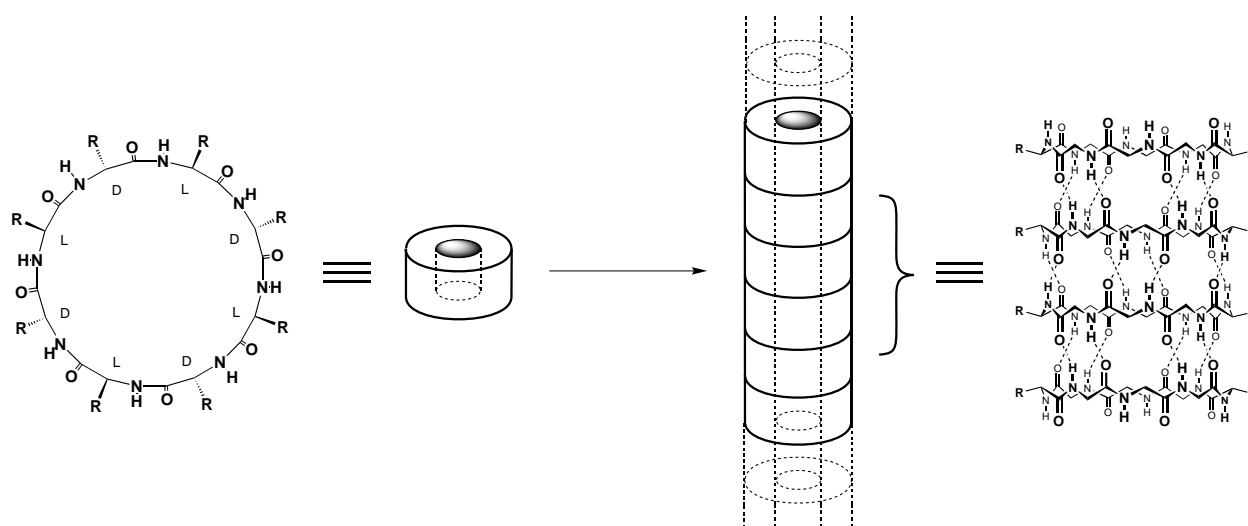
4. Ring-Stacking Motifs

4.1. Tubular Ensembles from Cyclic D,L- α -Peptides

4.1.1. Microcrystalline Peptide Nanotubes

Within the context of a theoretical analysis of regular enantiomeric peptide sequences, in 1974 DeSantis et al. recognized that peptides comprised of an even number of alternating D- and L-amino acids displaying conformationally equivalent β -type dihedral angles would form closed rings capable of stacking through backbone–backbone hydrogen bonding.^[29] The resulting hollow cylindrical ensembles are conceptually related to the β -helical conformations adopted by linear D,L-peptides (Figure 2).^[79–82] Initial attempts to experimentally demonstrate this type of tubular construct proved inconclusive.^[83] In 1989 an X-ray crystallographic study by Lorenzi and co-workers on the hexapeptides *cyclo*[-(L-Phe-D-Phe)₃-] and *cyclo*[-(L-Val-D-Val)₃-] revealed that the expected intersubunit associations were absent and each peptide was found instead to be tightly hydrogen bonded to several cocrystallized solvent molecules.^[84]

In 1993 our laboratory compellingly demonstrated the formation of hollow tubular structures by the stacking of cyclic D,L-peptide rings (Scheme 1).^[85] The sequence of octapeptide *cyclo*[-(L-Gln-D-Ala-L-Glu-D-Ala)₂-] was chosen to impart solubility in basic aqueous solution, and thereby to prevent subunit association through coulombic repulsion.



Scheme 1. Schematic diagram of nanotube assembly from cyclic D,L-peptides. For clarity, most of the peptide side-chains have been omitted.

Controlled acidification produced microcrystalline aggregates with high aspect ratios (length/thickness; Figure 5) that were examined by electron microscopy, electron diffraction,



Figure 5. Phase-contrast microscopy images of cyclic D,L-peptide nanotube microcrystals.

FT-IR spectroscopy, and crystal structure modeling. These analyses convincingly established the expected structure in which the ring-shaped subunits stack through antiparallel β -sheet hydrogen bonding to form hollow tubes with a van der Waals internal diameter of approximately 7 Å. Lambert and co-workers recently employed a similar pH-controlled assembly strategy to prepare microcrystals of a cyclic D,L-octapeptide containing bis-aspartic acid.^[86] The IR spectrum and morphology of the crystals formed by *cyclo*[-(L-Asn-D-Phe-L-Asp-D-Phe)₂-] were similar to those of *cyclo*[-(L-Gln-D-Ala-L-Glu-D-Ala)₂-] described earlier, which strongly suggests a tubular structure for this peptide.

One advantage of cyclic D,L-peptide nanotubes with respect to their β -helical counterparts is the possibility of rigorously controlling the internal diameter of the nanotube by simply varying the size of the peptide ring. A 1994 report from our laboratory demonstrated this design flexibility. The dodecapeptide *cyclo*[-(L-Gln-D-Ala-L-Glu-D-Ala)_n-] ($n=3$) was shown to undergo proton-triggered assembly in a manner

analogous to that previously described for its lower homologue ($n=2$).^[87] The resulting microcrystalline aggregates display an expanded van der Waals internal diameter of 13 Å.

Our laboratory has also prepared solid-state nanotubular assemblies using several uncharged cyclic octapeptides.^[88] For all cases reported from this laboratory, unit cell parameters obtained from cryoelectron microscopy and electron diffraction analyses are fully in accord with the expected tubular structures (Figure 6). Observed intersubunit distances of 4.8 Å strongly evince the anticipated β -sheet structures; furthermore, FT-IR spectroscopic studies reveal amide I_⊥, amide I_{||}, amide II_{||}, and hydrogen-bonded amide A bands which are characteristic of an antiparallel β -sheet arrangement. The low solubility of the cyclic D,L-peptide subunits and high stability of the resulting aggregates suggests significant preorganization of the monomeric units and a strongly cooperative assembly process. Recently, Karlström and Udén have explored association of cyclic D,L-octapeptides in water using a fluorescence-quenching assay. Their data indicate detectable intersubunit hydrogen bonding even in the strongly competing aqueous medium.^[89]

4.1.2. Self-Assembling Transmembrane Ion Channels and Pore Structures from Cyclic D,L- α -Peptides

A noteworthy feature of cyclic D,L-peptide nanotubes is the ease with which the external surface properties and internal diameter of the tubular ensemble may be altered through appropriate choice of amino acid side chains and the size of the peptide ring, respectively. For instance, in the design of transmembrane channels the ability to match the surface characteristics of nanotubes to the physical properties of the surrounding media proved of paramount importance. It was hypothesized that cyclic D,L-peptides bearing appropriate hydrophobic side chains would partition into nonpolar lipid bilayers and undergo self-assembly. In 1994 our laboratory validated this hypothesis by reporting the first self-assembling transmembrane ion channels based on the cyclic D,L-peptide nanotube framework (Figure 7).^[90] Since then several other

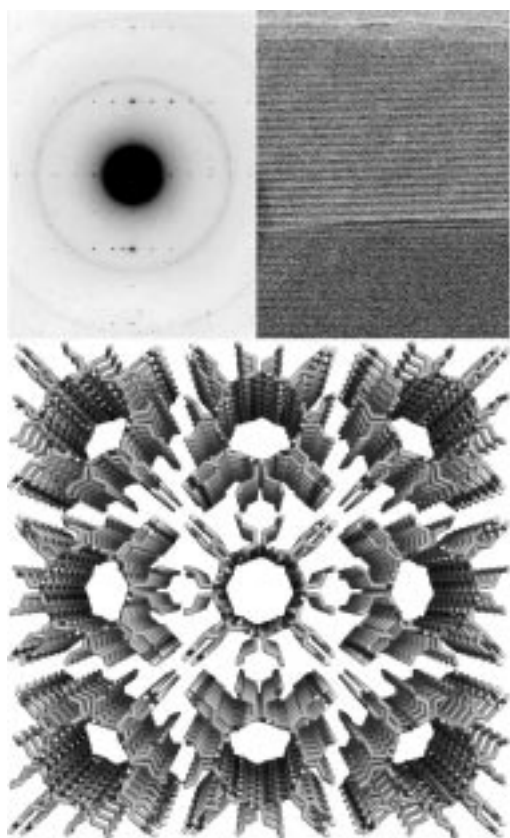


Figure 6. Bottom: Crystal-structure model calculated from electron microscopy for a cyclic D,L-peptide; nanotubular organization can be clearly seen. Top left: The corresponding electron diffraction pattern. Top right: A low-dose cryo-electron micrograph of the peptide microcrystals. Striations in the cryo-TEM image are approximately 18 Å apart; this corresponds to the diameter of a cyclic D,L-octapeptide and indicates side-by-side packing of the nanotubes in the solid state.^[85]

cyclic octapeptides have been examined by fluorescence proton-transport assays and single-channel conductance measurements.^[91] The self-assembling ion channels display transport activities for K^+ and Na^+ greater than 10^7 ions s^{-1} , rivaling the activity of the related natural product gramicidin A (Figure 7). More recently, grazing-angle reflection/absorption, polarized attenuated total reflectance (ATR), and transmission Fourier transform infrared (FT-IR) spectroscopic analysis of complexes formed from multiple lipid bilayers and peptides have shown that the nanotubes orient themselves nearly parallel to the lipid acyl chains, which supports our model of the peptide nanotubes as the active channel species.^[92]

As noted above, an important feature of cyclic D,L-peptide nanotubes is the ability to control the internal diameter by varying the ring size of the peptide subunit. Modeling studies suggested that subunits comprised of ten or more residues would form transmembrane pores large enough to mediate transport of small hydrophilic molecules across lipid bilayers. Consistent with these expectations, decapeptide *cyclo*[-(L-Trp-D-Leu)_n-L-Gln-D-Leu-] ($n=4$), which possesses a van der Waals internal diameter of 10 Å, displays efficient glucose transport activity, while its smaller octapeptide counterpart ($n=3$, internal diameter approximately 7 Å) lacks such

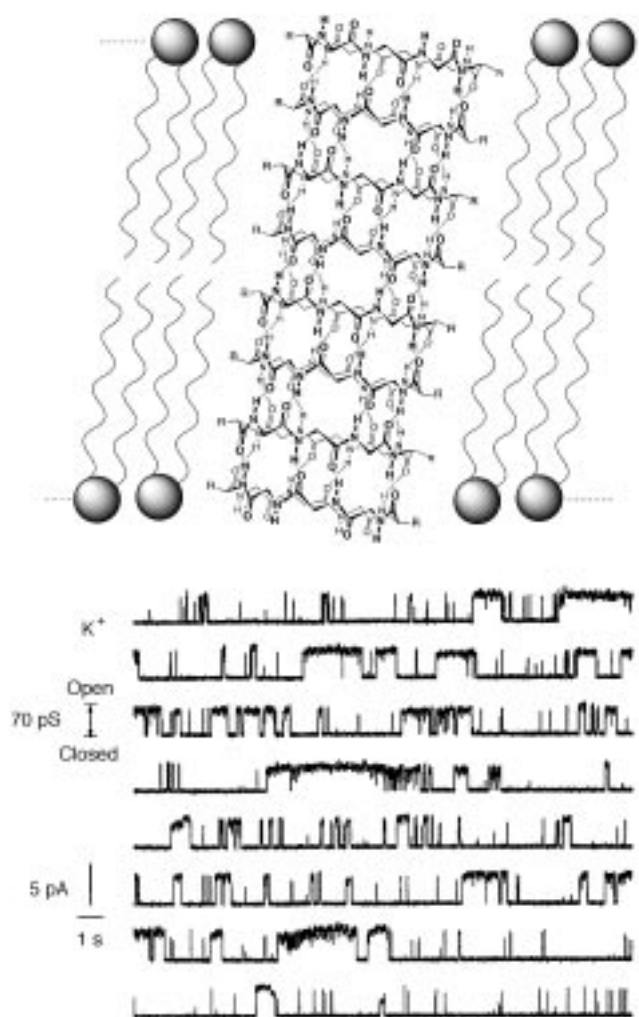


Figure 7. Top: Schematic representation of cyclic D,L-peptides assembled as a transmembrane channel. The off-normal tilt of the lipids and the peptide assembly are based on orientation studies using dichroic ATR-IR (ATR = attenuated total reflection).^[92] Bottom: Ionic conductance induced by the insertion of cyclic D,L-peptides into a voltage-clamped membrane.^[90]

activity.^[93] These findings suggest that even larger cyclic peptide subunits may prove useful in the delivery of pharmacologically active agents.

Cyclic D,L-octapeptide transmembrane channels have also been examined using computational methods. A model transmembrane channel structure was studied in our laboratory using molecular dynamics simulations. These results suggest that ordering of water molecules inside the channel lumen may be responsible for the observed high rates of ion transport (Figure 8).^[94] Using an Ohmic model of channel conductance together with an empirically derived correction factor, Smart and co-workers found that the observed channel conductance for *cyclo*[-(L-Trp-D-Leu)₃-L-Gln-D-Leu-] correlates well with the expected pore size.^[95] Based on Connolly surface-type calculations using the program HOLE, these authors reported a minimum internal diameter of 4.96 Å for the pore formed by the cyclic octapeptide, a result that contrasts with the 7 Å value reported earlier from our laboratory^[90] but that corresponds well with the anticipated 4.7 Å internal diameter of the related $\beta^{8.2}$ -helical structure.^[29] The discrepancy arises because the 7 Å value is derived from



Figure 8. Snapshot of a 0.76-ns molecular dynamics simulation of a stack of ten cyclic D,L-peptides in water.^[94] A section through the tube is shown, to reveal the relative organization of internal waters. Four types of orchestrated water movements were observed during the simulation that may contribute to the observed high rates of transport.

van der Waals rather than Connolly surface calculations; thus 4.96 Å and 7 Å probably represent the approximate minimum and maximum pore sizes, respectively.

4.1.2. Solution-Phase Tubular Assemblies from Cyclic D,L- α -Peptides

The fundamental translational repeat unit of cyclic D,L-peptide nanotubes comprises two subunits associated through antiparallel β -sheet hydrogen bonding. This minimal motif has been studied with the aid of selective backbone *N*-alkylation, which blocks one face of the peptide ring. In 1994 an X-ray crystallographic study of hemi-*N*-methylated hexapeptide *cyclo*[(-L^{Me}N-Leu-D-Leu)₃] by Lorenzi and co-workers provided the first atomic resolution information regarding cyclic D,L-peptide nanotube structure.^[96] This compound was shown to adopt the expected dimeric antiparallel β -sheet structure in the solid state, while NMR investigations revealed that the peptide dimerizes in deuterochloroform with an association constant of 80 M⁻¹.^[97] Independent work carried out in our laboratory demonstrated analogous solution and solid state dimerization by octapeptide *cyclo*[(-L-Phe-D^{Me}N-Ala)₄] (Figure 9).^[98] A recent study has examined the dimerization



Figure 9. Structure of a cyclic D,L-peptide (*cyclo*[-Phe-D^{Me}N-Ala]₄) in the crystal form (top and side views). This peptide is limited to dimer formation by *N*-alkylation of alternate amides.^[98] Alkylation prevents further oligomerization driven by hydrogen bonding. The cylindrical cavity is filled with partially disordered water molecules.

of twenty cyclic D,L- α -peptides varying in location and identity of backbone alkyl substituents, amino acid composition, and ring size.^[55] Our findings establish that, of the various ring sizes examined, cyclic octapeptides exhibit optimal rigidity and predisposition for nanotube assembly. A variety of *N*-alkyl substituents were tolerated, for example, methyl, allyl, *n*-propyl, and pent-4-en-1-yl groups. In addition, initial

findings suggest that residues with γ -branched side chains favor dimerization over those with unbranched side chains, presumably by predisposing the peptide backbone for β -sheet formation.

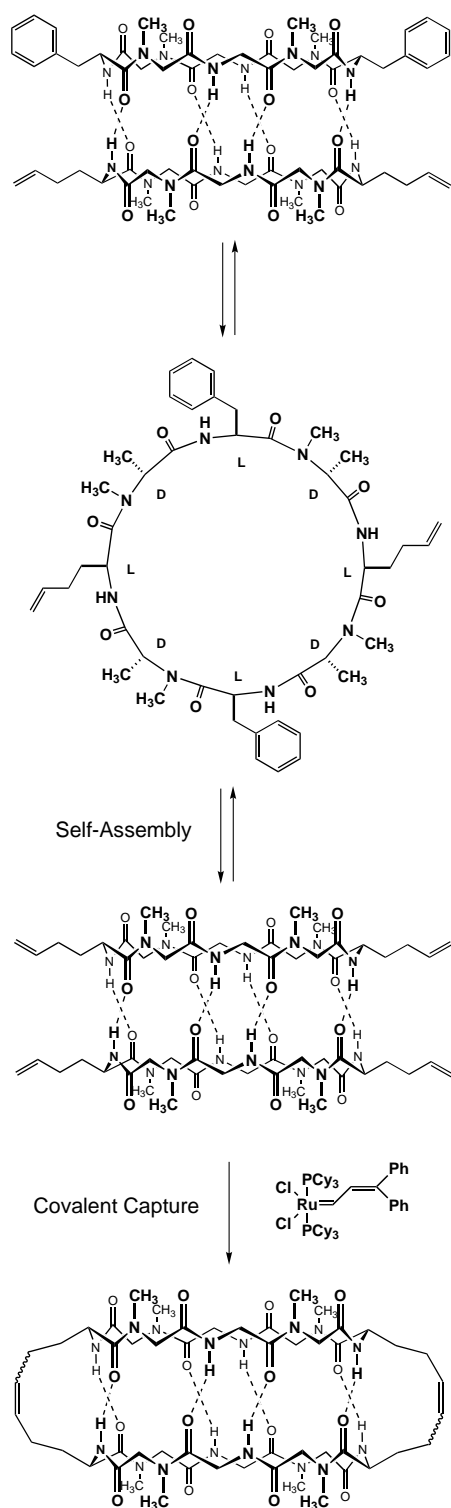
Self-assembling peptide cylinders have also provided the first experimental model system for assessment of the relative stability of parallel and antiparallel β -sheet structures.^[99] Measurement of solution equilibrium constants revealed that antiparallel orientation is favored over parallel by 0.8 kcal mol⁻¹. Results from independent computational studies corroborate these findings.^[100, 101]

In model studies directed toward preparation of polymeric tubular biomaterials, the feasibility of covalently capturing noncovalent cyclic peptide dimers has been examined. Octapeptide *cyclo*[-(L-Phe-D^{Me}N-Ala-L-Hag-D^{Me}N-Ala)₂] bearing two olefin groups underwent selective olefin metathesis mediated by hydrogen bonds to yield the corresponding covalently tethered β -sheet peptide dimer (Scheme 2).^[102] Recent work has employed disulfide isomerization to extend the scope of this general strategy.^[103] In the two peptide systems examined, intersubunit hydrogen bonding serves important yet distinct functions. In the case of olefin metathesis, hydrogen bonding appears to drive the reaction by increasing local concentration of olefin functionalities. In contrast, for disulfide isomerization, hydrogen bonding appears to control partitioning between two alternative disulfide-bonded dimers by contributing to the stability of the hydrogen-bonded isomer. Our proposed mechanism (Scheme 3) for the latter transformation is reminiscent both of thiol-catalyzed “unscrambling” of RNase A and oxidative refolding pathways of natural proteins and protein fragments.

4.2. Tubular Ensembles from Cyclic Peptides Containing β -Amino Acids

In 1972 Hassall hypothesized that cyclic tetramers of alternating α - and β -amino acids would assemble through backbone–backbone hydrogen bonding to yield hollow cylindrical constructs.^[104] A crystallographic study of tetrapeptide *cyclo*[-(L-Ser(OrBu)- β -Ala-Gly- β -Asp(OMe))₄] in 1974 only partially validated this proposal.^[105] The peptide subunits adopted a ring-shaped conformation and stacked above one another in the crystal lattice; however, only two of the four amide groups participated in expected intersubunit hydrogen bonding.

While the design of tubular assemblies employing mixed α - and β -amino acid cyclic peptides awaits definitive demonstration, cyclic peptides composed of all β -amino acids have already found application in preparation of hollow tubular assemblies.^[106, 107] Seebach and co-workers have reported that cyclic tetrapeptides composed solely of chiral β^3 -amino acids can form hollow tubular structures similar to those displayed by cyclic D,L- α -peptides.^[106] Molecular modeling based on X-ray powder diffraction data has indicated that tetrapeptides *cyclo*[-(β^3 -(S)-HAla)₄], *cyclo*[-(β^3 -(S)-HAla- β^3 -(R)-HAla)₂], and *cyclo*[-(β^3 -(S)-HAla)₂-(β^3 -(R)-HAla)₂] all exhibit tubular structures in the solid state (Figure 10). Recently our laboratory demonstrated ion channel formation by two cyclic β^3 -



Scheme 2. Schematic illustration of the covalent capture of a cyclic peptide dimer using olefin metathesis. The peptide *cyclo*[-(Phe-D^{Me}N-Ala-Hag-D^{Me}N-Ala)₂-] self-assembles in solution to provide two interconverting dimers in equal proportions (Hag = homoallylglycine). Only the complex in which the homoallyl side-chains are directly across from each other can undergo metathesis to form the covalent product.^[102] Reprinted with permission from ref. [102]. Copyright (1995) American Chemical Society.

tetrapeptides (Figure 11).^[107] Fluorescence proton transport experiments and single-channel conductance data indicate ion-channel activities similar to those of cyclic D,L- α -peptides,

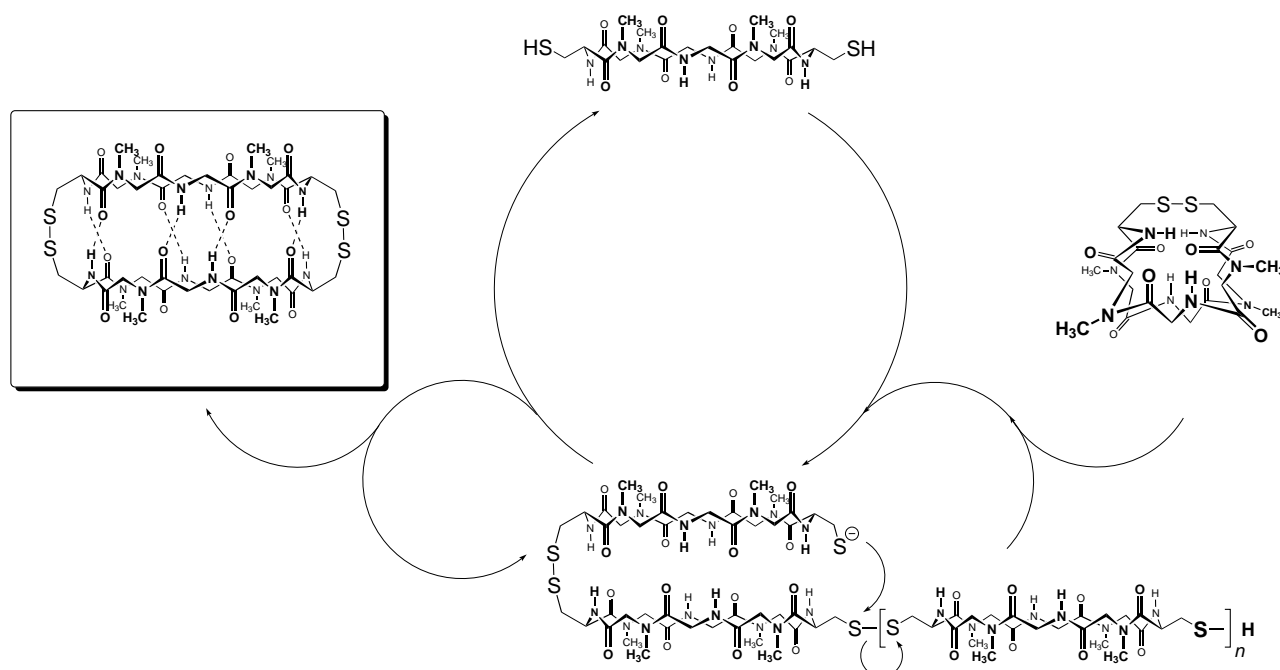
with K⁺ transport rates of 1.9×10^7 ions per second. Channel-forming cyclic β^3 -peptides are also expected to exhibit unique properties distinct from those of their D,L- α -peptide counterparts. For example, the unnatural β^3 -peptide backbone has been shown to cause uniform alignment of amide groups in the solid state structure of *cyclo*[-(β^3 -(S)-HAla)₄-] (Figure 10).^[106] Analogous alignment of amide groups in the proposed channel structures should give rise to a macrodipole moment reminiscent of an α -helix. This dipole is expected to influence the conductance of cyclic β^3 -peptide ion channels by causing voltage gating and current rectification behavior. In contrast, the alternating directionality of amide functionalities in cyclic D,L- α -peptide nanotubes causes local dipole moments to be cancelled out; therefore no voltage gating or current rectification behavior is expected for these channel structures.

4.3. Cystine Macrocycles

The foregoing examples of ring-stacking motifs employ symmetrical cyclic subunits displaying a high degree of self-complementarity due to the formation of multiple noncovalent intermolecular contacts. Ranganathan, Karle et al. have explored the assembly properties of less symmetric macrocycles, and found that very few specific recognition sites are required to induce in-register macrocycle stacking. Their studies have focussed on macrocycles composed of *n*-alkanes (from butyl to decyl) that bridge a cystine moiety either as bisamides^[108] or bisureas.^[109] These compounds were expected to be macrocyclic hosts for lipophilic guests, and indeed, when the bisureas are treated with α,ω -alkane dicarboxylic acids, their chloroform solubility increases dramatically, suggesting that carboxylate recognition disrupts aggregation by inducing urea conformations parallel to the ring plane. This supposition was confirmed by ¹H NMR studies.^[109] Surprisingly, despite the demonstrated conformational flexibility of the macrocycle, these molecules organize in the solid state to form tubular arrays with open molecular pores in which cystines are on one side of the tube and alkane loops form the other side of the tube. The central pores are roughly rectangular and range from 5–10 Å on the long axis and 4–4.5 Å on the shorter axis. Two molecules within a stack are stitched together through two hydrogen bonds in the bisamide and four hydrogen bonds in the bisurea. Additional aggregation free energy probably arises from the hydrophobic collapse of the alkyl region of the tube. As expected, these amphiphilic tubes assemble in the lattice to optimize molecular packing, however, when possible, the hydrophobic side of a single tube is completely buried against other hydrophobic tube faces.

4.4. Serinophanes

Ranganathan et al. have also recently reported studies on an aromatic cyclodepsipeptide based on serine (serinophane), which also stacks to form crystalline cylindrical assemblies.^[110] Interestingly, the amide hydrogen-bonding functionality is directed into the plane of the ring, preventing its participation



Scheme 3. Minimal mechanism for disulfide exchange in *cyclo*[-(Phe-D-MeN-Ala-Cys-D-MeN-Ala)₂-]. The intramolecular cystine first experiences intermolecular thiol–disulfide exchange to give the linear oligomer. When $n \geq 1$, intramolecular disulfide exchange yields the thermodynamically favored dimeric species.

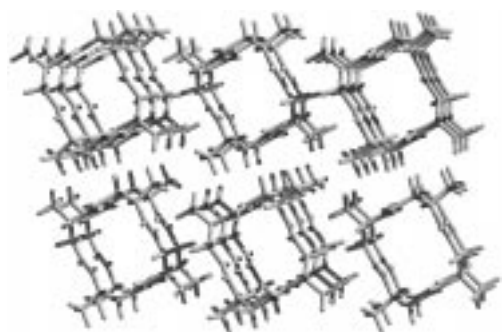


Figure 10. Crystal structure of the cyclic β -peptide, *cyclo*[-(β^3 -(S)-HAla- β^3 -(R)-HAla)₂] that shows the formation of tubular peptide arrays.^[106]

in intermolecular tubular aggregation. Instead, the assembly is driven by aromatic π -stacking of pyridyl and phenyl rings (Figure 12), similar to the phenylacetylene macrocycles (see Section 4.6). However, adjacent rings in a column do not come into direct van der Waals contact; rather, the phenyl rings of surrounding columns interdigitate to form intertubular zipper-like structures. Structural analysis also showed alternation in the stack between phenyl and pyridyl rings. Notably, while the phenyl–pyridyl and dipyril serinophanes formed channel structures, the diphenyl compound did not display π -stacked structures at all, underscoring the subtlety of weak molecular recognition motifs. This aromatic flat-ring peptide system, as well as Moore's phenylacetylene oligomers (see Section 4.6), may well be suitable for exploring other well-defined aromatic interactions, such as phenyl–perfluorophenyl recognition^[111–113] or cation– π -induced stacking.^[114–118]

4.5. Carbohydrate Nanotubes

In 1992 a report by Harada, Li, and Kamachi described preparation of a novel cyclodextrin polyrotaxane by threading a single polyethylene glycol bisamine (PEG-BA) molecule through several cyclodextrins, then stoppering the amine ends with dinitrofluorobenzene.^[119] A later study described an elegant extension of this methodology in which the templated rotaxane assembly was covalently cross-linked using the biselectrophilic reagent epichlorohydrin (Scheme 4).^[120] Subsequent destoppering and purification by gel filtration afforded the polymeric nanotubular structure. The identity of the product was confirmed by NMR, IR, and UV spectroscopies, and by gel filtration analysis. Given the well-known tendency of cyclodextrins to form inclusion complexes, these tubular polymers are expected to exhibit interesting host–guest behavior. Similarly, recent reports have described oligomeric “nanotube” inclusion complexes between cyclodextrins and α,ω -diphenylpolyenes.^[121–123] However, the resulting complex is not stable in the absence of a polyene guest, and are perhaps more properly classified as polypseudorotaxanes.

The polysaccharide backbone itself has inherent conformational preferences, depending on the linkage pattern. This is strikingly demonstrated by the hollow, helical form adopted by α -amylose, which is a regularly repeating polymer of glucose. The curvature of this linear polymer is a direct consequence of the $\alpha(1 \rightarrow 4)$ linkage and results in a helical pore; indeed, iodine stains starch by filling this molecular cavity with iodine.^[124, 125] Employing an efficient polycondensation–cycloglycosylation strategy, Stoddart and co-workers have recently prepared the cyclic variant of coiled oligosaccharides in a series of novel cyclodextrin analogues from

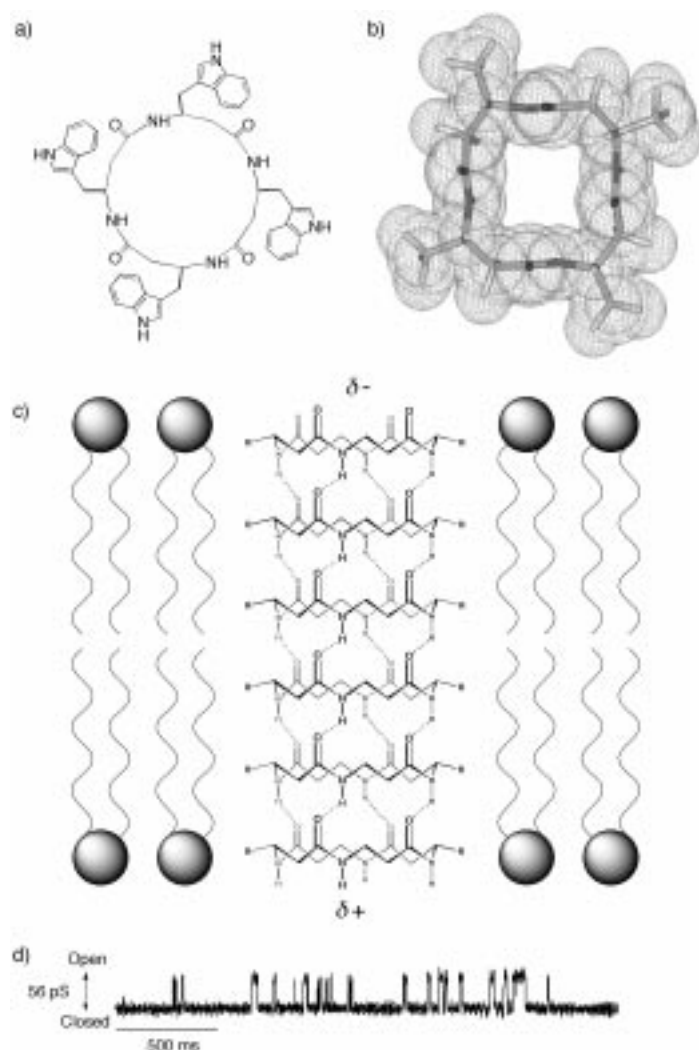


Figure 11. a) Schematic illustration of a cyclic β^3 -tetrapeptide, $cyclo\text{-(}\beta^3\text{-HTrp)}_4$, designed to form a transmembrane ion channel. b) Molecular model of the channel-forming β^3 -peptide, with surface rendering indicating the 2.6–2.7 Å open pore. c) Illustration of the transmembrane insertion of the cyclic peptide assembly, which displays the expected parallel ring-stacking. d) Single-channel K^+ conductance trace induced by cyclic β^3 -peptide and recorded at 60 mV.^[107] As with the cyclic D,L- α -octapeptides, the opening and closing events may reflect rapid peptide assembly–disassembly events in the membrane.

protected disaccharide precursors.^[126–128] Initial work focused on cyclic (1 \rightarrow 4)- α -linked oligomers of L-rhamnopyranose–(1 \rightarrow 4)- α -D-mannopyranose. Trityl cation catalyzed cyclo-oligomerization of trityl/cyanoethylidene-activated disaccharide followed by deprotection afforded good yields of cyclic hexa- and octameric products. X-ray crystallographic analysis revealed that the octamer adopts a C_4 -symmetrical conformation in the solid state and stacks to form hollow tubular structures with internal diameters around 1 nm (Figure 13).^[126] Following a similar procedure, achiral oligomers of D- and L-rhamnopyranose (RP) as well as D- and L-mannopyranose (MP) were prepared and characterized.^[127] The resulting cyclic hexasaccharide (from MP), octasaccharide (from RP), and decasaccharide (from RP) gave X-ray diffraction quality crystals. The structures of the octa-

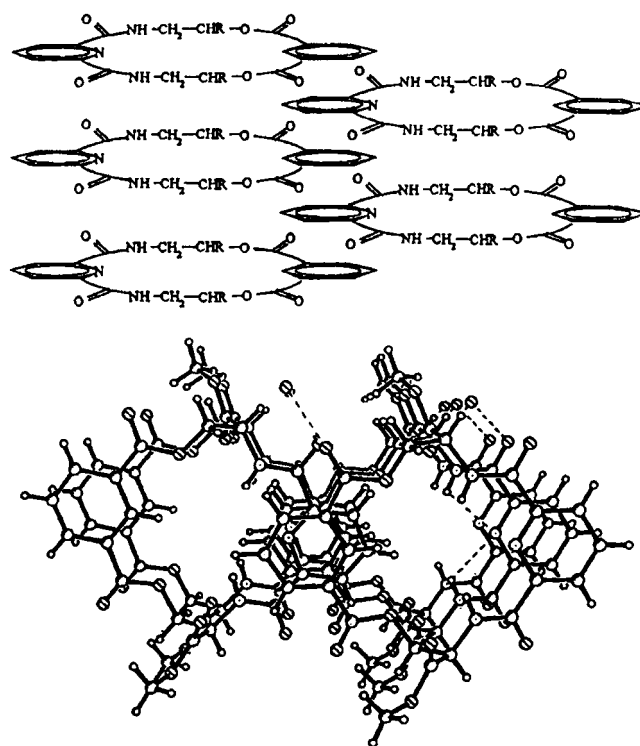


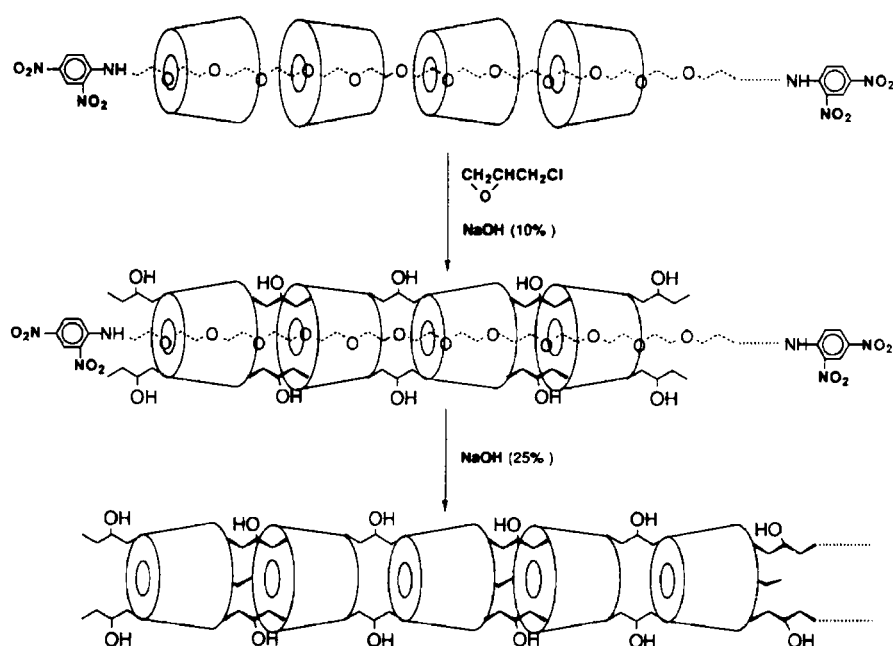
Figure 12. Top: A schematic depiction of the stacking interactions in the solid-state structure of a cyclic depsipeptide (serinophane). Note the alternate stacking of pyridyl and phenyl rings of adjacent serinophane columns. Bottom: The crystal structure of the same depsipeptide, which reveals the interdigitated aromatic rings and the 2.35 Å open channel through the assembly.^[110] Reprinted with permission from ref. [110]. Copyright (1998) American Chemical Society.

saccharide^[127] and the decasaccharide^[128] were tubular, while the hexasaccharide (from MP)^[128] formed a parquet-like superstructure. In all cases, included solvent molecules were observed within the macrocyclic cavities, which suggests the possibility of interesting host–guest properties for these structures.

4.6. Phenylacetylene Macrocycles

Zhang and Moore have examined the liquid crystalline behavior of shape-persistent phenylacetylene macrocycles (PAMs).^[129] Based on the previously documented propensity of PAMs with electron-withdrawing ester substituents to self-associate in solution,^[130, 131] similar long-chain alkyl analogues were initially examined. These compounds were found to be incapable of disordering into isotropic liquid crystals, presumably due to numerous favorable π -stacking interactions. However, differential scanning calorimetry (DSC) and X-ray diffraction (XRD) analysis of isomeric acylated phenolic PAMs revealed both discotic nematic and columnar phases consistent with tubular ring stacking.^[129] Modeling indicated that the expected tubular structures possess an internal hydrogen to hydrogen distance of approximately 8 Å.

In related work, Moore and co-workers have studied the solid-state assembly of PAMs bearing hydrogen-bonding functionalities.^[132] X-ray crystallographic analysis revealed that the phenolic derivative forms two-dimensional hydrogen-



Scheme 4. Formation of a cyclodextrin nanotube by covalent capture of a polyrotaxane precursor. Treatment of the noncovalent assembly with epichlorohydrin captures the cyclodextrins to yield a molecular tube that is unoccluded after removal of the poly(ethylene glycol) thread.^[120] Reprinted with permission from *Nature* **1993**, 364, 516–518. Copyright (1993) Macmillan Magazines Ltd.

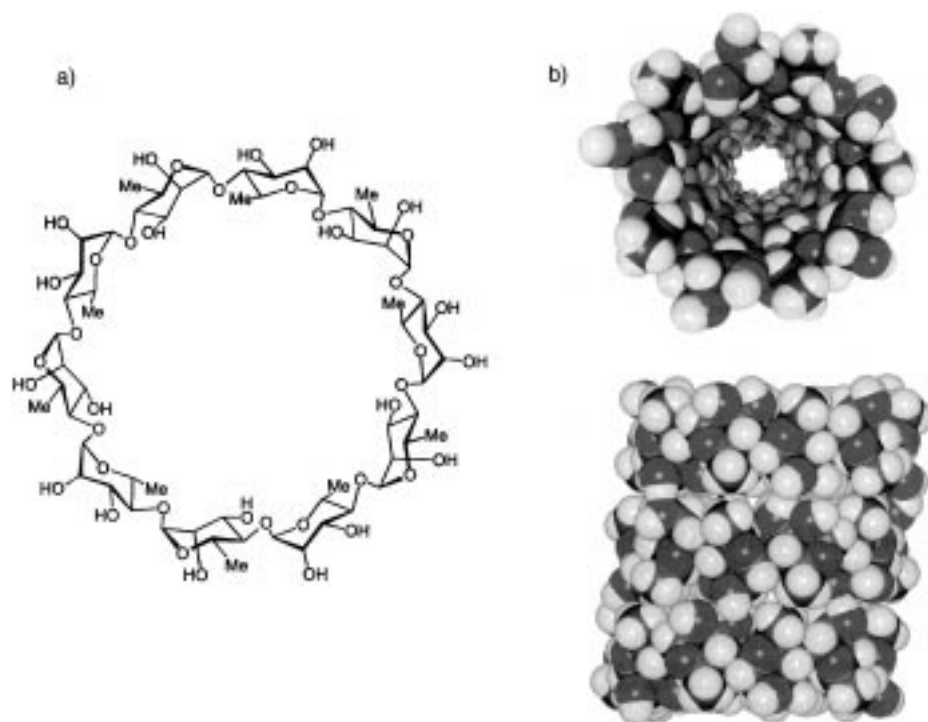


Figure 13. a) Chemical structure of cyclic D,L-rhamnopranose, which forms a solid-state tubular structure. b) Views along the cylindrical axis (top) and perpendicular to the cylindrical axis (bottom).^[126]

bonding networks which stack so as to maintain registry between the macrocyclic cavities (Figure 14). The resulting extended channel structures are filled with solvent molecules. In principle, properties such as pore size and solvophilicity can be varied by covalent modification of PAM precursors.

4.7. Tubular Mesophases from Macrocyclic Precursors

In 1985 a report from Lehn and co-workers described the first attempts at preparing liquid crystals exhibiting columnar phases consisting of stacked macrocyclic molecules.^[133] A number of cyclic hexaamines bearing long-chain *N*-alkyl substituents were synthesized. Results from XRD analyses of the resulting mesophases proved consistent with the expected columnar mesomorphic order. A model was proposed involving supramolecular arrangement of the macrocyclic mesogens into parallel, hollow columns. Later XRD analysis of brominated analogues confirmed the anticipated hexagonal columnar mesomorphism, which strongly supports the proposed tubular structures.^[134]

5. Sector-Assembly Motifs

The previous sections have detailed ways in which macrocycles and coiled molecules can self-organize into tubular materials by virtue of their well-defined shape. In those examples, cylindrical shape is immediately apparent from the monomeric species; pore size is defined by the degree of coiling or the ring size. A more complex approach to tubular constructs relies on the non-covalent assembly of wedge- or sector-shaped subunits to create molecular curvature. Conceptually, such an approach is similar to the stacking of molecular discs; however, this strategy demands higher order self-assembly as the discs are now separated into many sectors. This assembly topology^[135] has been visually demonstrated in Whitesides and co-workers' exploration of mesoscale assembly^[135] as well as in his earlier studies on the construction of molecular "rosettes", formed from the molecular recognition of melamine with cyanuric acid.^[135–138] Notably, the bismelamine–bisocyanuric acid variant of this self-assembly system forms "nanorods" through polymerization mediated by hydrogen bonds, although it is unclear whether or not an internal pore is formed upon polymerization.^[139]

Interestingly, this elaborate sector approach to tubular materials can be executed using perhaps the simplest possible starting materials as molecular sectors: lipids. Lipids are

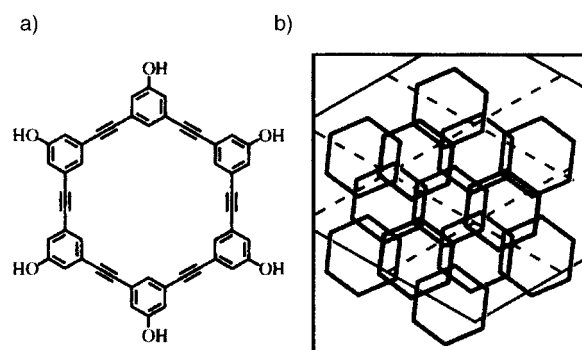


Figure 14. a) Chemical structure of the nanotube-forming phenolic acetylene macrocycle. b) Schematic representation of the crystal packing in the crystal structure. The macrocycles form a two-dimensional hexagonal closest packing which is reinforced by hydrogen bonding between phenolic substituents on adjacent macrocycles.^[132] Reprinted with permission from *Nature* **1994**, 371, 591–593. Copyright (1994) Macmillan Magazines Ltd.

among the most common biological amphiphiles, typically composed of long hydrocarbon chains coupled to a polar headgroup. Variations within this basic framework alter the lipid molecular shape, which allows lipid assemblies to access a wide range of structural morphologies, from micellar and hexagonal (H_{II}) phases to the lamellar (L_a) structure found in biomembranes (Table 1).^[140–142] The formation of these different structures in aqueous media is driven by exclusion of water, which provides the aggregate in which hydrocarbon chains are most efficiently close-packed against one another while the polar headgroups remain exposed to the solvent. Cylindrical structures have been formed from lipids that assemble in both lamellar and nonlamellar topologies. Although a detailed understanding of lipid aggregate topology requires quantitative thermodynamic consideration,^[140–143] a qualitative rationalization of aggregate morphology can be derived from evaluation of the molecular dimensions of the

individual lipid (Table 1). Lipid molecular shape can be generally described by three parameters: S_0 is the area of the polar headgroup, l is the maximum molecular length, and v is the molecular volume of the hydrophobic domain.^[144] The quotient v/IS_0 is called the *critical packing parameter*; essentially, it is the ratio of the interfacial area of the hydrophobic and hydrophilic regions. If $\frac{1}{2} \leq v/IS_0 \leq 1$, then the lipid is approximately cylindrical and a low-curvature aggregation topology such as the L_a bilayer phase provides optimum burial of the hydrophobic surface area and is therefore favored to form. Similarly, if $v/IS_0 \leq \frac{1}{3}$, then the polar head of the amphiphilic molecule is larger than its nonpolar domain, the molecular shape is inverse conical, and the formation of micellar-type aggregates with the polar headgroups exposed and the nonpolar regions packed against one another will be favored. Conversely, if $v/IS_0 > 1$, then the nonpolar region of the amphiphile is larger than the polar domain, the molecular shape is the cone, and a hexagonal (H_{II}) phase can be formed. Thus, lipid choice allows a measure of control over the consequent aggregate morphology.



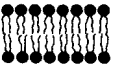

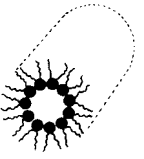

5.1. Assembly of Disc Sectors: Hexagonal Lipid Phases

The earliest reported examples of tubular lipid assemblies are represented by lipids in the inverse hexagonal phase. Lipids with a high spontaneous curvature (that is, a “wedge” shape) are especially likely to form these tubular phases, in which ordered polar headgroups line water-filled columns that are insulated from one another by disordered hydrophobic lipid tails (Table 1). Like many lipid phases, the formation of this phase is highly dependent on lipid shape and conditions, such as temperature, pressure, concentration, and extent of hydration,^[145, 146] which can strongly influence the diameter of these water-filled channels. Researchers have sought to capture these self-assembled porous materials by phase polymerization with varied methods.^[147] O’Brien and co-workers have worked extensively with modified lipids which bear the naturally occurring phosphoethanolamine headgroup and dienoyl functionality in the lipid tail;^[148] the small phosphoethanolamine head group and unsaturated acyl chains dictate hexagonal phase formation while the dienes allow for phase polymerization by addition of redox initiators at elevated temperatures.

5.2. Inverse Hexagonal Phases from Artificial Amphiphiles

The general concepts revealed from the study of structure–phase relationships displayed by natural lipids can be readily applied to artificial systems in which a specific three-dimensional order is desired. Percec and co-workers have pioneered studies on the behavior of amphiphiles based on a gallate core (Figure 15) in which the three phenoxy groups are alkylated with hydrophobic functionalities while the 1-carboxyl group is rendered hydrophilic through esterification or ionization, to yield a wedge-shaped molecule that readily forms a hexagonal columnar liquid-crystalline phase (see refs. [149–152] and

Table 1. Molecular shapes and critical packing parameters v/IS_0 for some lipids are shown, as well as the expected phase morphology that arises from particular shapes.^[142] Reprinted with permission from ref. [142]. Copyright (1989) Springer New York.

Lipid	Phase	Molecular shape	v/IS_0
lysophospholipids detergents	 micellar	 inverted cone	$< \frac{1}{3}$ (sphere)
phosphatidylcholine sphingomyelin phosphatidylserine phosphatidylinositol phosphatidic acid cardiolipin digalactosyldiglyceride	 bilayer	 cylinder	$\frac{1}{3}$ to $\frac{1}{2}$ (globular shapes; rods)
phosphatidylethanolamine (unsaturated) cardiolipin – Ca^{2+} phosphatidic acid – Ca^{2+} (pH < 6.0) phosphatidic acid (pH < 3.0) monogalactosyldiglyceride	 hexagonal (H_{II})	 cone	> 1

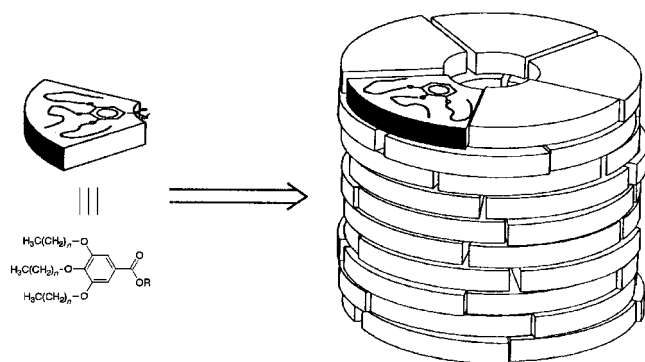
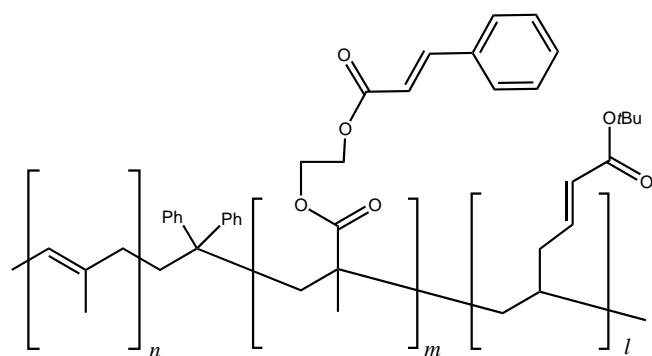


Figure 15. Schematic depiction of the assembly of a hexagonal phase from a synthetic amphiphile derived from gallic acid. The sector shape of the trialkylated gallate results in the formation of columnar liquid-crystalline arrays.^[149]

references therein). These molecules apparently assemble in a discotic fashion with the hydrophilic benzoate groups pointing towards one another in the center of the “disc”. Indeed, when the gallic acid nucleus is esterified with oligoethylene glycols the hexagonal phase is stabilized by the addition of lithium and sodium salts, as judged by increased phase transition temperatures from the hexagonal phase to the isotropic phase (melting).^[153] This suggests that the metals cooperatively bind to multiple gallate derivatives in the center of the self-assembled column, though they may also stabilize the assembly by enhancing hydrophobic interactions.

5.3. Nanotubes from Block Copolymers

Recent work from Stewart and Liu demonstrates another approach towards tubular nanostructures. By using a triblock copolymer of the type shown in Scheme 5 composed of



Scheme 5. Chemical structure of a triblock copolymer, in which the ratio of isoprene, cinnamoyl ethyl methacrylate, and *tert*-butyl acrylate is approximately 1:1:6; $n = 130$, $m = 130$, $l = 800$.^[154]

polyisoprene, poly(2-cinnamoyl ethyl methacrylate), and poly(*tert*-butyl acrylate) blocks in an approximate 1:1:6 ratio, they formed cylindrical micelles with an isoprene core. The assembly was then cross-linked with UV light to provide a stable covalent structure. The polyisoprene core, unreactive with UV light, was then decomposed by ozonolysis to yield a hollow tube of cross-linked acrylate polymer.^[154] The cylin-

drical micelles appear to be approximately 65 nm in diameter, as observed by transmission electron microscopy (TEM) when the micelles were stained with RuO_4 . Compelling evidence for tube formation is afforded by increased electron transmission in the center of the polymer strands after ozonolysis; a light-colored stripe is seen running down the middle of each strand, suggestive of a hollow interior (Figure 16). Interestingly, the authors were apparently able to fill the tubes by treatment with rhodamine B dye, which restores the TEM absorbance levels to those prior to ozonolysis.

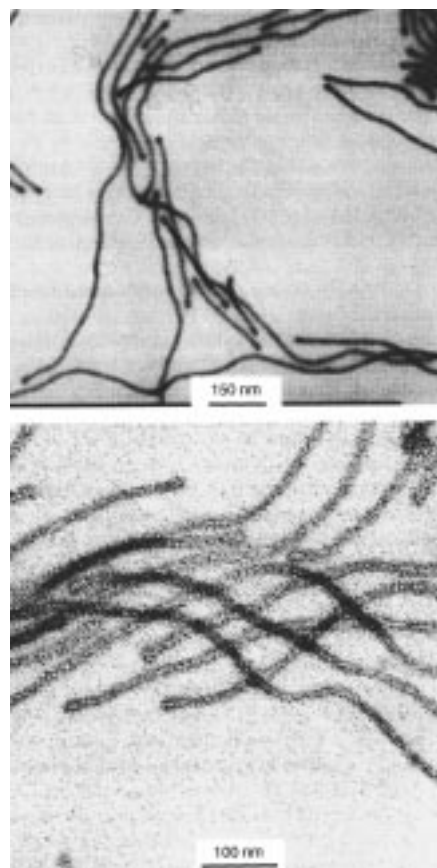


Figure 16. TEM images of cylindrical micelles of the triblock polymer from Scheme 5), before (top) and after (bottom) ozonolysis of the isoprene core. The micelles (top) were stained with OsO_4 and the ozonolysed product with RuO_4 . The lighter core of the ozonolysed micelle suggests the formation of polymeric tubes.^[154]

6. Folded-Sheet Motif

Lipid tubules composed of bilayer sheets curled into cylinders have been observed in various surfactant systems, derived from amino acids,^[155–157] galactocerebrosides,^[158] and other unnatural lipids. Particular attention has been given to the tubular lipid assemblies formed from the synthetic lipid 1,2-bis(tricoso-10-12-diynoyl)-*sn*-glycerol-3-phosphocholine, which bears a zwitterionic headgroup and diacetylenic unsaturation in each hydrocarbon chain. Yager and Schoen first reported in 1984 that a suspension of this lipid in alcohol–water mixtures results in the spontaneous formation of tubular structures upon cooling below the lipid melting

temperature.^[159, 160] These cylindrical aggregates were found to be composed of curved bilayer sheets in which the lipid chain axis is perpendicular to the cylinder axis (Figure 17). Moreover, these constructs were hollow and open-ended with

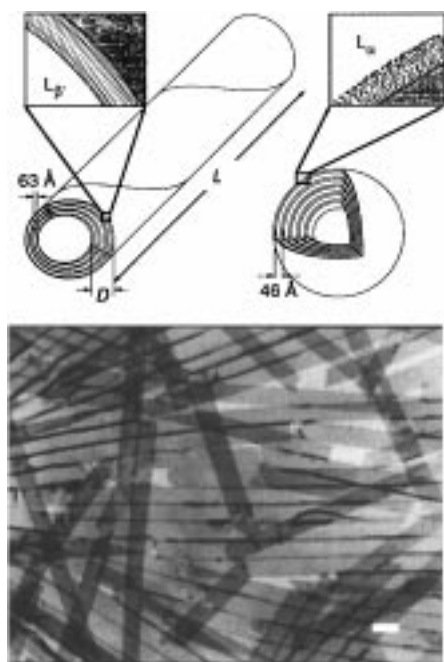


Figure 17. Top: Schematic depiction of the differences in lipid packing of lipids with diacetylenic groups in the hydrophobic section and natural fluid-phase lipids (D = thickness, L = length of the tube). The first case results in tubule formation and the second in spherical liposome formation. The rigid shape of the diacetylenic lipids induces a bilayer curvature which leads to tubule formation, whereas the fluid natural lipids are much more disordered, resulting in a more symmetric spherical lipid morphology. Bottom: Negatively stained electron micrographs of single bilayer 1,2-bis(tricosyl-10,12-diinoyl)-*sn*-glycero-3-phosphocholine tubules in methanol/water.^[167] Tubule diameter is approximately 0.75 μm .

a typical diameter of 0.5 μm and lengths ranging from 50–200 μm . Varying self-assembly conditions such as temperature, lipid concentration, and solvent can control lipid tubule size. When methanol is used as the aqueous cosolvent at low lipid concentrations, unilamellar (single-walled) tubules are formed,^[161] whereas an ethanol/water lipid suspension consists of largely multilamellar tubules, with 5–10 bilayers per tubule wall.^[162] Additionally, spherical multilamellar vesicles (MLVs) and cylindrical MLVs (tubules) are found on the same thermal landscape with the spherical liposomes occupying the higher temperature regime; thus heating and cooling lipid suspensions allow for reversible cycling between the two morphologies.^[160] Interestingly, the length of tubules formed is closely linked to the cooling rate of lipid suspensions from the spherical MLV regime, and therefore it is possible to control both tubule wall thickness and tubule length to some degree.^[163]

The origin of tubule formation is not entirely understood, though the bilayer curvature required for cylinder formation is probably a result of unique packing requirements caused by the diacetylene functionality in the lipid acyl chains. This surface curvature apparently induces a preferential lipid

orientation that has the ultimate consequence of twisting the bilayer to form an optically active lipid aggregate.^[164, 165] Indeed, the tubules exhibit a significant Cotton effect when analyzed by CD spectroscopy,^[166, 167] whereas the spherical MLVs do not provide a detectable dichroic signal. Furthermore, freeze–fracture electron microscopy revealed a right-handed helical twist in each tubule, demonstrating the chiroselective nature of assembly.^[160]

While much effort has been devoted to the stabilization of these lipid assemblies since first reported by Yager and Schoen in 1984, diyne polymerization-phase capture does not appear to be a viable strategy as the enyne polymeric product has considerably different conformational requirements than the curved bilayer. There have been accounts of successful capture of the tubule shape through use of the lipid assembly as a template for the deposition of more rugged materials, such as nickel, copper, or magnetic alloys.^[168]

7. Potential Applications

7.1. β -Helical Biosensors

Gramicidin A has been exploited in a novel biosensor apparatus that capitalizes on the dimeric state of the active β -helix channel.^[169] In this system, biomolecule recognition (that is, antibody–antigen binding) is coupled to either an increase or decrease in the number of active channel species in a solid-supported lipid bilayer (Figure 18). A gramicidin peptide is

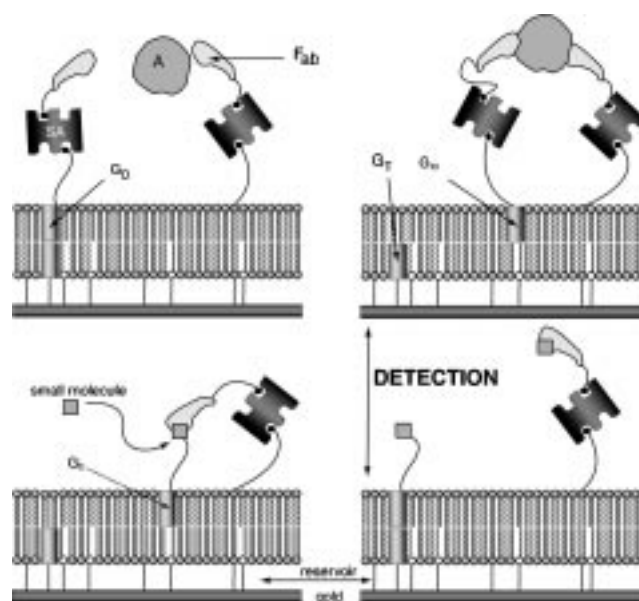


Figure 18. Schematic representation of an ion-channel switch biosensor.^[169] A lipid bilayer is tethered onto a gold surface by sulfur–gold bonds between the thiol-terminated membrane-spanning lipids and the surface. Gramicidin molecules are similarly surface tethered (G_r) and stochastically interact with free gramicidins (G_a or G_b) that diffuse into the upper bilayer; this forms conducting gramicidin dimers (G_D). The conducting dimers report the binding of a small molecule to a membrane-bound receptor (antibody fragment F_{ab}) by an increase in conductance (bottom, left to right). The disruption of the dimer, and therefore a drop in conductance, (top, left to right) reports the binding of antigen A by cross-linking the membrane-bound receptor and a gramicidin-bound receptor.

covalently bound to the gold support through a linker thiol–gold bond, as are some fully membrane-spanning lipids, which serve to stabilize the bilayer. Another gramicidin peptide is also incorporated into the membrane, and is not bound to the support, but is instead functionalized with a biomolecular recognition element, such as an antibody or antigen. This second peptide diffuses freely in the top monolayer, occasionally recognizing the lower monolayer gramicidin peptide and opening a channel, which can be detected by electrical conductance measurements. An identical antibody or antigen is similarly attached to a support-anchored lipid, and thus when a bivalent analyte (molecule A) binds, the diffusing gramicidin peptide is bound, the channel is broken, and conductance stops (Figure 18, top). When a competing analyte is added to the medium, the gramicidin is freed, the channel restored, and the conductance resumes (Figure 18, bottom), thereby allowing the detection of small molecule analytes.

In preliminary studies aimed at preparing ion selective membranes, Roemer, Lorenzi, and Weisenhorn have examined thin films of the synthetic $\beta^{4,4}$ -helical oligopeptide Boc-D-Val-(L-Val-D-Val)₇-OMe. These authors found that, at low surface pressures, Langmuir films of the peptide lie flat at the air–water interface, while at higher pressures the peptide reorients itself with its helical axis perpendicular to the surface of the water.^[170] Atomic force microscopy (AFM), ellipsometry, and grazing angle IR measurements of Langmuir–Blodgett films supported on ultraflat silicon surfaces corroborated these conclusions.^[171]

7.2. Biosensors from Cyclic D,L-Peptides

As an approach toward the design of diffusion-limited sensors, cyclic eight-residue D,L- α -peptides have been assembled into oriented tubular structures and supported in organosulfur self-assembled monolayers (SAM) on gold films (Figure 19).^[172, 173] The structural properties of SAM-supported peptide nanotubes have been analyzed by grazing-angle

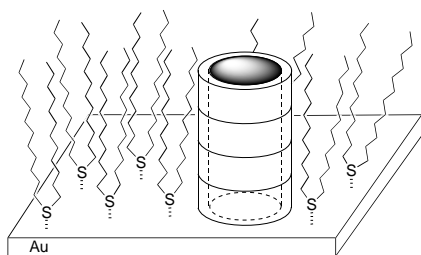


Figure 19. Schematic depiction of a biosensor similar to that in Figure 18 which is based on cyclic D,L-peptides. A gold surface enjoys protection by a monolayer of thioethers that is punctuated by cyclic peptide stacks. These stacks would then allow the size-selective sensing of ions in solution.^[173]

FT-IR and their functional properties by cyclic voltammetry and impedance spectroscopy. These studies have demonstrated the feasibility of diffusion-limited size-selective ion sensing based on supported tubular biomaterials.

7.2.1. Small-Molecule Detection with Cyclic D,L-Peptide Adapters

Recent work from the Bayley laboratory has demonstrated the utility of a natural pore-forming protein as a molecular biosensor. Bayley and co-workers have coupled small-molecule (or ion) binding events to the flow of electrical current through a single molecular channel in a membrane. Thus, a molecular recognition event can be dramatically amplified above background electrical noise and be detected with exquisite sensitivity. Previously, genetic engineering of the heptameric toxin α -haemolysin to incorporate metal-binding ligands into the lumen of the molecular channel allowed the quantitative detection of various divalent metal ions in solution.^[174] However, small-molecule detection using the haemolysin channel proved to be a less tractable problem as it was not clear how to design a substrate binding pocket into the lumen structure. To address this, a cyclodextrin molecule was used as a “molecular adapter”, which fits snugly within the cylindrical lumen of haemolysin, coaxial with the protein pore (Figure 20). Thus, all molecules flowing through the haemolysin channel were filtered through the cyclodextrin molecular adapter.^[175] This allowed researchers to detect the small molecules that bound to cyclodextrin and blocked ion flow, which was registered as a decrease of channel conductance (Figure 21).

In an effort to find molecular adapters that are more readily tailored to detect a broader range of substrates, cyclic D,L-octapeptides were studied for their ability to noncovalently modify haemolysin and detect small-molecule substrates. These cyclic peptide adapters possess a clear advantage over the cyclodextrins in that the functionality presented at the pore aperture is easily altered by changing the amino acid sequence. In this fashion, the sensor selectivity can be manipulated by choice of peptide adapter, rather than the decidedly more involved process of engineering the protein pore itself. Furthermore, the facility of cyclic peptide synthesis renders chemical libraries of peptides accessible so that adapters for a wide range of substrates may be readily found. This approach takes advantage of the relatively sequence-independent flat-disc shape of cyclic D,L-peptides; not only does this rigid shape predispose the peptides towards self-assembly, but it provides a reliable platform for the presentation of chemical functionality (Figure 20d). A recent examination of this peptide-modified ion-channel biosensor system has shown that various polyanionic small organic molecules (Figure 20e) can be detected, including the second messenger inositol triphosphate (IP₃).^[176] Clearly, this biosensor system demonstrates how tubular shape can be flexibly controlled in order to maximize chemical selectivity.

7.3. Antibiotic Properties/Targeted Cytotoxicity

We note that self-assembling cyclic D,L-peptide nanotubes exhibit significant *in vitro* antibacterial activities and may therefore serve as lead compounds in the development of new antimicrobial and cytotoxic agents.^[177] Attachment of bulky groups to the cyclic peptide side chains has been shown to

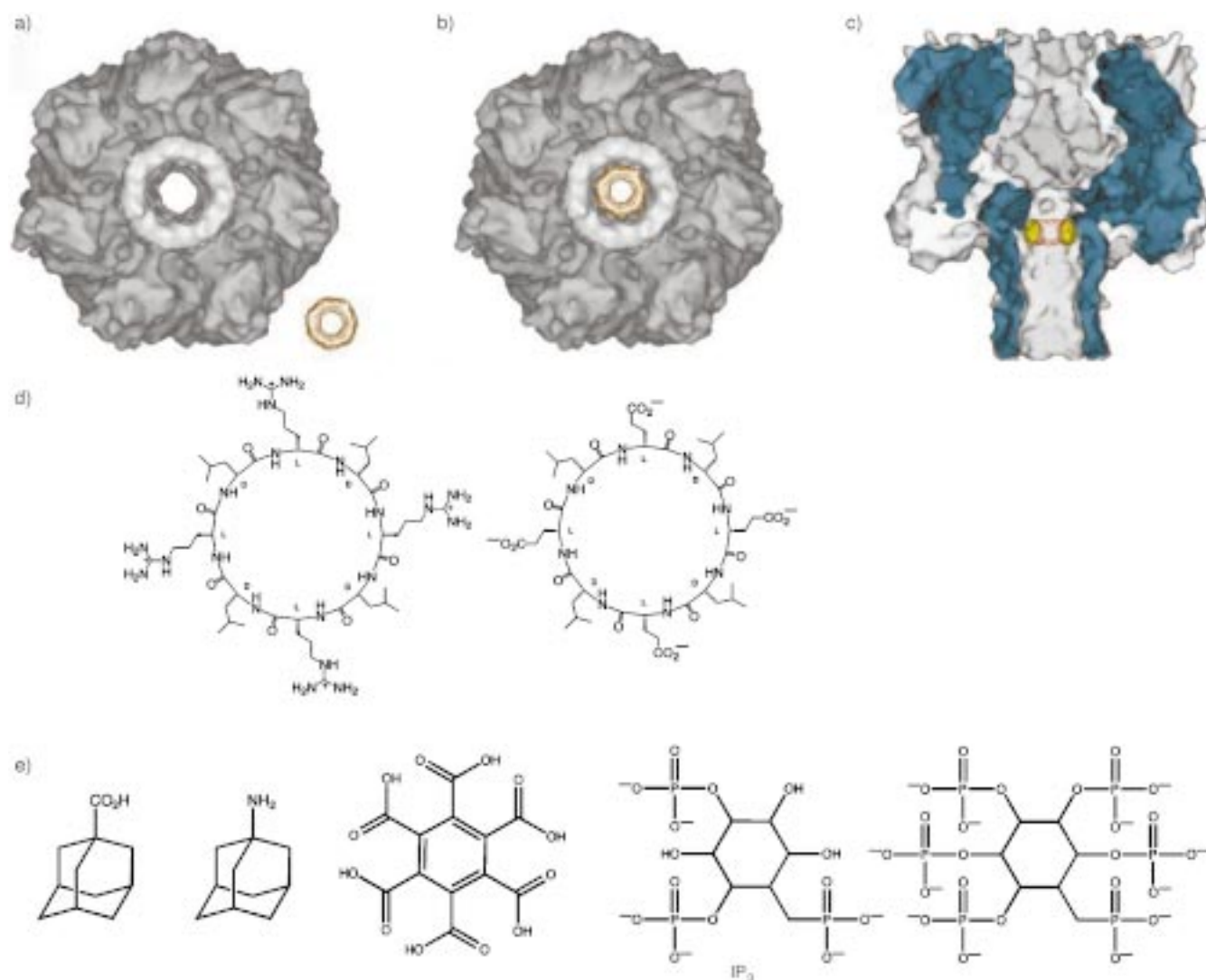


Figure 20. a)–c) Molecular graphics representations of the interaction between α -haemolysin (HL) and β -cyclodextrin as a molecular adapter. a) View along the pore axis without adapter. b) View along the pore axis with an inserted adapter. c) View of a sagittal section of the heptameric HL pore, with the adapter in place, where it is expected to be lodged at a site of constriction of the pore.^[175] d) Chemical structures of the cyclic D,L-peptide molecular adapters used to detect small polyanionic molecules (e). Reprinted with permission from *Nature* **1999**, 398, 686–690. Copyright (1999) Macmillan Magazines Ltd.

sterically inhibit ring stacking and therefore channel formation, suggesting the possibility of derivatizing the cyclic peptide subunits with a specific cell-targeting motif through an enzymatically labile bond. Cleavage of the targeting group at the specific cell-recognition site would create a high concentration of active peptides, thereby favoring channel formation and leading to disruption of transmembrane gradients. Furthermore, the nonnatural alternating D,L-configuration may increase the bioavailability of these peptides by enhancing their resistance to proteolytic degradation.

7.4. Electronic Properties

Recently, several computational studies employing density functional methods have focused on elucidating the electronic properties of cyclic-D,L-octapeptide nanotubes. The results of Takeda and co-workers suggest that intersubunit hydrogen bonding may delocalize electrons and holes toward the tube

axis, so that band conduction might occur through the interring hydrogen bonds.^[178] More recently, Takeda and co-workers have examined the role of intra- and inter-ring hydrogen bonds in determining the electronic structure of peptide nanotubes and found that the electronic band-edge states are strongly dependent on the inter-ring hydrogen bonds.^[179] Employing calculations with gradient-corrected exchange-correlation potentials, Carloni et al. have predicted a large gap in the low-energy electronic excitation spectrum, with both extended and localized states near the gap.^[180] These findings are supported by the results of Lewis et al., which indicate a HOMO–LUMO gap of approximately 5 eV for the nanotube structure, consistent with a transparent material and suggesting interesting bioelectronic device applications for the cyclic peptide nanotube systems.^[181] Jishi et al. have calculated a 4.62 eV HOMO–LUMO gap and found that the nanotubes are insulators that could function as inert vessels in which foreign guest atoms may be incorporated.^[182]

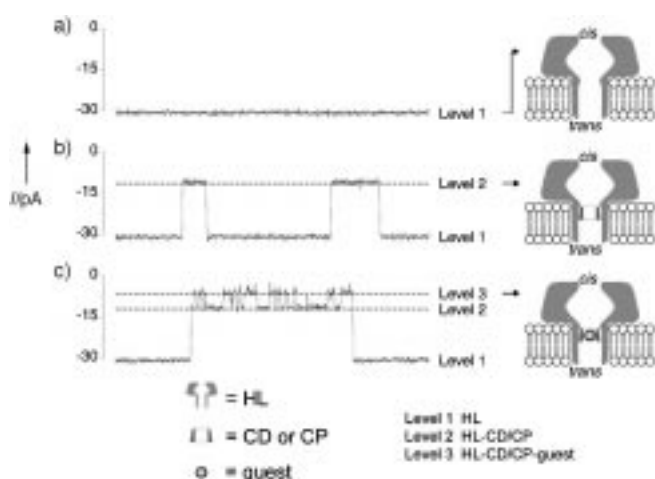


Figure 21. Conductance measurements for a bilayer, which demonstrate the utility of α -hemolysin with a molecular adapter as a small-molecule biosensor. Level 1 indicates the conductance across a membrane modified with only α -hemolysin (HL), level 2 indicates the decreased conductance level caused by binding of a molecular adapter within the HL lumen, and level 3 indicates the further reduction in conductance caused by stochastic binding of guests to the molecular adapter while it is bound inside the HL channel. The data shown correspond to experiments using β -cyclodextrin as an adapter^[175] and adamantamine hydrochloride as a guest; similar results have been found using cyclic D,L-peptides (CP; Figure 20d) as adapters. Reprinted with permission from *Nature* **1999**, 398, 686–690. Copyright (1999) Macmillan Magazines Ltd.

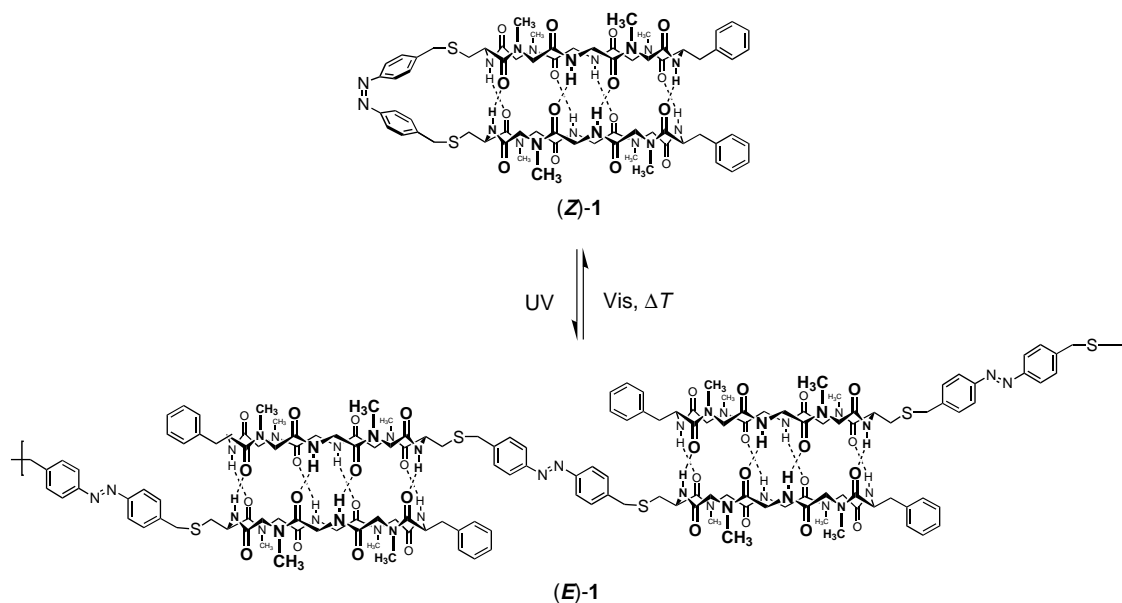
7.5. Photoresponsive Materials

Much research has been devoted to the study of molecules whose physical properties can be reversibly switched using light.^[183–189] Such systems are expected to be of great utility in the synthesis of read-write-erase optical data storage devices, as well as in “smart polymers”.^[190] For these applications, two significantly different and stable molecular states that are bridged by distinct light inputs are required. This would provide a state-switchable system in which the signal-to-noise

ratio (that is, the difference between states 1 and 2) is maximized. Thus, efforts have been made to couple secondary protein-folding with light-induced transitions, as the cooperative folding process is an all-or-none phenomenon that separates two very distinct states: compact, folded peptide and random-coil, unfolded peptide.^[191] Nucleation of certain peptide motifs such as a turn of an α -helix is known to rapidly induce the folding process.^[192, 193] Thus, if critical turn conformations could be reversibly controlled by light, one would then arrive at an efficient photo-switchable peptide system that could be radiatively folded and unfolded and possibly employed in the aforementioned applications.

Recent work in our lab has been directed towards such photoswitchable systems. Building upon studies of covalently captured cyclic D,L-peptides, we have examined a covalent dimeric system in which the two cyclic peptides are connected through an azobenzene spacer (Scheme 6).^[194] The peptides were further modified by *N*-methylation of alternate amides, restricting the hydrogen-bonding capability to one face of each flat-ring peptide. Modeling indicated that only the *Z* conformation of the azobenzene would permit intramolecular hydrogen bonding between the two linked peptides, to form a cylindrical dimer, whereas the *E* conformation would prevent close intramolecular interactions and would result in the formation of noncovalent hydrogen-bonded oligomers of azo-linked peptides. The *E* \rightarrow *Z* and *Z* \rightarrow *E* isomerizations were induced by irradiation at 366 nm and visible light, respectively. Conversion between *Z* and *E* yields an 85:15 ratio at the photostationary state. As expected, intramolecular hydrogen bonding enhanced the stability of the *Z* form, resulting in a rare quantitative *E* \rightarrow *Z* transition. Furthermore, kinetic experiments revealed that the thermal isomerization in the dark from *Z* \rightarrow *E* was 7.5 times slower in the peptide system than with 4,4'-dimethylazobenzene.

Although this system proved to be highly reversible in solution, it was unclear whether or not there would be enough



Scheme 6. Schematic illustration of the azo-linked cyclic D,L-peptide dimer and its light- and heat-mediated equilibria between the monomeric *cis* isomer and the oligomeric hydrogen-bonded *trans* isomer.^[194]

free volume to allow isomerization in the solid state. Thus, we further examined the behavior of these linked dimers in two-dimensional solids, or Langmuir thin films.^[195] Both isomers readily formed stable films, which were more robust than those produced with monomeric, nonalkylated cyclic peptides.^[196] Indeed, similar photoisomerization reversibility was found in thin films. However, though both *E* and *Z* isomers have a similar area/molecule, scanning force microscopy revealed that the *E* isomer is predisposed to form molecular bilayers, whereas the *Z* isomer prefers to pack in a monolayer. Thus, significant differences in surface pressure arise upon isomerization; essentially, the system undergoes a reversible and substantial change in organization properties upon exposure to specific light wavelengths. Further development in this promising system may therefore lead to smart materials that could change their macroscopic properties in response to light.

7.6. Biomaterials

Our laboratory has also investigated the formation and stabilization of transition metal nanoclusters (quantum dots) on the surface of cyclic D,L-peptide nanotubes.^[197] These studies were inspired by natural biomineralization processes which are thought to require the display of oriented functionalities on protein and oligosaccharide templates. Indeed, similar work has been done using the functionalized surfaces of lipid tubules to template crystallization of minerals.^[198] In preliminary studies the organized array of carboxylic acid groups on the crystalline surface of a peptide nanotube was used to nucleate the room temperature deposition of nearly monodispersed (approximately 3 nm large) copper(I) oxide nanoclusters (Figure 22). The resulting nanocomposite material was characterized by high-resolution TEM and electron energy loss spectroscopy (EELS). The regular presentation of functionality of the tube surface may also provide a useful substrate for the crystallization of minerals.

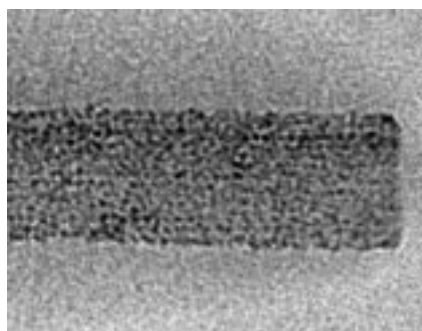
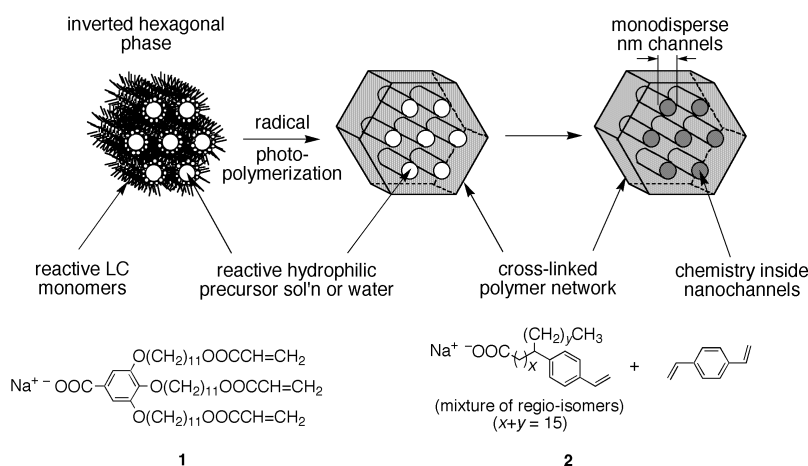


Figure 22. High resolution cryo-TEM of a copper oxide nanocomposite deposited on a *cyclo*[-Gln-D-Ala-Gln-D-Ala-]₂ self-assembled microcrystal. The copper(I) clusters have an average radius of 1.5 nm.^[197]

7.7. Ordered Nanocomposites

Although Percec has demonstrated the ability of metal substrates to bind to the decorated columnar interior of hexagonal phases from gallate-based mesogens (see Section 5.2), the tubular core of this hexagonal phase was first fully exploited by Gin and co-workers, who prepared defined polymer–polymer nanocomposites of a gallate-based hexagonal phase and poly(*p*-phenylenevinylene) (PPV) in which the PPV threaded the channel at the center of the gallate column.^[199] Gin and co-workers' modifications of the gallate platform incorporated acrylate functionality at the end of the phenoxy hydrophobic tails as well as the sodium salt of gallic acid, to allow formation of the hexagonal phase as an aqueous suspension (Compound **1**, Scheme 7). When this mesogen was

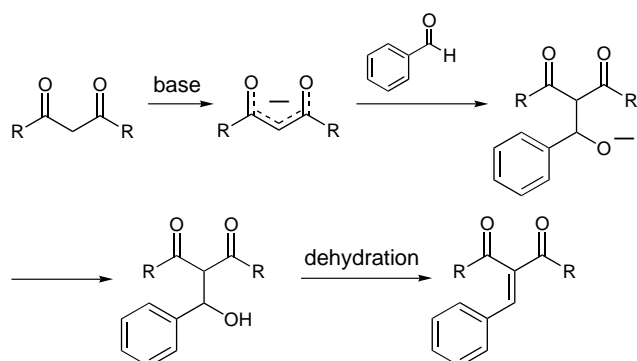


Scheme 7. Synthetic approach to nanocomposite materials using polymerizable inverse hexagonal liquid-crystalline phases. Compounds **1** and **2** are known to form inverted hexagonal phases that can be photocross-linked (with or without divinyl benzene) to capture the columnar arrangement of amphiphiles with water-soluble substrates trapped inside the nanometer scale channels.^[199, 205]

mixed with a water-soluble PPV precursor, the PPV precursor occupied the aqueous channel lined by the benzoate functionalities. Subsequent photoinitiated polymerization of the acrylate groups allowed for covalent phase capture of the nanocomposite while thermal treatment yielded the mesogen-insulated PPV material. The resulting PPV fluorescence is enhanced approximately four times over pure PPV, which indicates potent protection from self-quenching mechanisms^[200, 201] by the chain-dilution effect of the nonfluorescent matrix, although there may be other factors involved. The authors have also demonstrated the effective encapsulation of transition metal and lanthanide ions to introduce new properties into these nanocomposites. Composites with europium ions enhanced Eu^{III} luminescence due to the small degree of hydration of the composite core, although self-quenching through diffusion along the cylindrical axis is still possible. (For organic systems designed to site isolate Eu^{III} for the purposes of luminescence enhancement, see refs. [202, 203].) Thus, this method uses the cylindrical nature of the hexagonal phase to synthesize nanostructured materials in a fashion that appears quite general for preparing columnar arrays of water-soluble substrates.^[199, 204]

7.8. Chemical Catalysis

Gin and co-workers have further utilized the polymerization phase-capture strategy to obtain tubular materials that can catalyze the Knoevenagel condensation of ethyl cyanoacetate with benzaldehyde (Scheme 8).^[205] This catalytic power



Scheme 8. Hann–Lapworth mechanism of the Knoevenagel condensation.

is direct result of the cylindrical assembly. Using a carboxylate amphiphile (Compound **2**, Scheme 7) they have been able to form cylindrical micelle assemblies in which the water-filled pores of 10–15 Å diameter are lined with carboxylate groups. Addition of divinylbenzene and subsequent photocross-linking results in polymerization phase-capture of this tubular array. The enforced proximity of the carboxylates causes strong electrostatic repulsion and drives a substantial increase in the pK_a value^[206–209] to 5 pK units above the value for the free carboxylate in water. This renders the carboxylates into effective weak bases, which are known to catalyze the Knoevenagel condensation.^[210] The influence of local environment on chemical reactivity has been thoroughly exploited by enzymes and has also been demonstrated in other regular micellar and monolayer systems.^[211–214] Gin and co-workers' incorporation of these concepts into open, porous, and covalent structures provides a reasonable platform for exploration of organic heterogeneous catalysis, or "organic zeolitic" catalysts.^[205]

7.9. Slow-Release Drug Delivery

Price and co-workers have examined the possibility of using diyne lipid bilayer tubules or the "folded-sheet" tubes discussed earlier as slow-release drug-delivery vehicles, since the aqueous channels can readily be filled with water-soluble molecules. The high aspect ratio of these tubes renders them less sensitive to damage from osmotic pressure as the molecules are released. This principle was first tested with tetracycline, which was found to be released slowly over several months.^[215] Price then applied tubule-controlled release to address the problem of marine bio-fouling. To do this, tubules were coated with copper and dried to form microcapillary tubes,^[216] mixed with an antifouling epoxy resin, then painted onto fibreglass rods, which were exposed

to marine conditions. In contrast to a heavily fouled control rod with only the epoxy resin mixed with paint, the tubule-treated rod remained clean after six months of exposure,^[23, 217] indicating that tubular materials may be very useful for controlled release applications.

8. Summary and Outlook

A number of approaches to organic nanotubes have been presented in recent years. Some, like the β -helical channels, may require the context of a hydrophobic matrix such as a lipid bilayer to be useful. Steric compression caused by the syndiotactic backbone of β -helices provides the impetus of cylinder formation, but helical pitch remains difficult to control. In contrast, the *meta*-substituted phenylacetylene oligomers are well suited for reliable helical-cylinder formation, as the turn angle is rigidly fixed, and only one helical pitch can provide sufficient solvophobic backbone burial. However, it seems that these linear systems are limited to low-oligomer tubular states, which may decrease their potential applications. In both these systems, large entropic gains are made upon cyclization, which result in readily-formed solid-state tubular arrays of stacked phenylacetylene macrocycles, oligosaccharides, and cyclic D,L-peptides. In the cyclic form, pore size becomes well-defined and controllable. Thus, design of function is greatly facilitated; one has a reliable repeat unit that can be exploited to place functionality in a supramolecular lattice with molecular precision. Possible applications for such nanotubular structures are many and range from preparation of novel cytotoxic and controlled-release drug-delivery agents to catalytic and materials science applications, such as biomineralization and site isolation of chromophores or other reactive groups. Stacked cyclic molecules must utilize specific modes of self-assembly to assemble—however, in the cited examples, relatively simple and robust scaffolds of molecular recognition have been employed with great success. In the more fluid lipid systems, even simpler and less-specific recognition motifs are employed. Hydrophobic collapse of amphiphiles can result in extremely complex tubular arrays that are liquid crystalline in nature, yet very stable. Again, the pore size of these arrays is difficult to predict and may depend on dispersion conditions. As our collective understanding of the factors affecting self-assembly of macromolecules and amphiphiles grows, it seems likely that much of the future work in tubular assemblies will focus on cyclic and "sector" approaches, or combinations thereof, to cylindrically organized, and increasingly functional materials.

We would like to thank our co-workers for the past eight years for their insightful contributions to our efforts in the area of self-assembling peptide nanotubes: D. Bashford, L. K. Buehler, J. Buriak, R. Chadha, A. Chavoshi, E. Choi, M. Delgado, M. Engels, J. Eppinger, S. Fernandez, J. D. Hartgerink, M. P. Isler, A. Janshoff, N. Khazanovich, H. S. Kim, K. Kobayashi, K. Kraehenbuehl, G. V. Long, D. E. McRee, R. A. Milligan, K. Motesharei, J. Sanchez-Quesada, C. Steinem, N. Tamaoki, M. S. Vollmer, and K. Wilcoxon. We are also grateful

for the financial support of the Office of Naval Research (Dr. Harold Bright, Program Director), Department of Defense, and National Institute of Health (Grant no.: GM 52190).

Received: July 6, 2000 [A419]

- [1] B. Eisenberg, *Acc. Chem. Res.* **1998**, *31*, 117–123.
- [2] P. B. Sigler, Z. Xu, H. S. Rye, S. G. Burston, W. A. Fenton, A. L. Horwich, *Annu. Rev. Biochem.* **1998**, *67*, 581–608.
- [3] A. L. Horwich, E. U. Weber-Ban, D. Finley, *Proc. Natl. Acad. Sci. USA* **1999**, *96*, 11033–11040.
- [4] P. Zwickl, D. Voges, W. Baumeister, *Philos. Trans. R. Soc. London B* **1999**, *354*, 1501–1511.
- [5] D. Voges, P. Zwickl, W. Baumeister, *Annu. Rev. Biochem.* **1999**, *68*, 1015–1068.
- [6] M. Borgnia, S. Nielsen, A. Engel, P. Agre, *Annu. Rev. Biochem.* **1999**, *68*, 425–458.
- [7] J. S. Lindsey, *New. J. Chem.* **1991**, *15*, 153–180.
- [8] D. Philp, J. F. Stoddart, *Angew. Chem.* **1996**, *108*, 1242–1286; *Angew. Chem. Int. Ed. Engl.* **1996**, *35*, 1154–1196.
- [9] S. Iijima, *Nature* **1991**, *354*, 56–58.
- [10] P. M. Ajayan, T. W. Ebbeson, *Rep. Prog. Phys.* **1997**, *60*, 1025–1062.
- [11] M. Estermann, L. B. McCusker, C. Baerlocher, A. Merrouche, H. Kessler, *Nature* **1991**, *352*, 320–323.
- [12] C. T. Kresge, M. E. Leonowicz, W. J. Roth, J. C. Vartuli, J. S. Beck, *Nature* **1992**, *269*, 710–712.
- [13] A. Monnier, F. Schüth, Q. Huo, D. Kumar, D. Margolese, R. S. Maxwell, G. D. Stucky, M. Krishnamurty, P. Petroff, *Science* **1993**, *261*, 1299–1303.
- [14] G. D. Stucky, Q. Huo, A. Firouzi, B. F. Chmelka, S. Schacht, I. G. Voigt-Martin, F. Schüth, *Stud. Surf. Sci. Catal.* **1997**, *105*, 3–28.
- [15] L. Song, M. R. Hobough, C. Shustak, S. Cheley, H. Baley, J. E. Gouaux, *Science* **1996**, *274*, 1859–1866.
- [16] T. Schirmer, T. A. Keller, Y.-F. Wang, J. P. Rosenbusch, *Science* **1995**, *267*, 512–514.
- [17] S. W. Cowan, T. Schirmer, G. Rummel, M. Steiert, R. Ghosh, R. A. Pauptit, J. N. Jansonius, J. P. Rosenbusch, *Nature* **1992**, *358*, 727–733.
- [18] M. S. Weitz, G. E. Schultz, *J. Mol. Biol.* **1992**, *227*, 493–509.
- [19] E. A. Merritt, S. Sarfaty, F. Vandenakker, C. Lhoir, J. A. Martial, W. G. J. Hol, *Protein Sci.* **1994**, *3*, 166–175.
- [20] D. A. Doyle, J. M. Cabral, R. A. Pfuetzner, A. Kuo, J. M. Gulbis, S. L. Cohen, B. T. Chait, R. MacKinnon, *Science* **1998**, *280*, 69–77.
- [21] R. R. Ketchum, W. Hu, T. A. Cross, *Science* **1993**, *261*, 1457–1460.
- [22] A. Klug, *Angew. Chem.* **1983**, *95*, 579–596; *Angew. Chem. Int. Ed. Engl.* **1983**, *22*, 565–582.
- [23] R. R. Price, M. Patchan, A. Clare, D. Rittschof, J. Bonaventura, *Recent Dev. Biofouling Control* **1994**, 321–334.
- [24] D. Caspar, K. Namba, *Adv. Biophys.* **1990**, *26*, 157–185.
- [25] K. Namba, G. Stubbs, *Science* **1986**, *231*, 1401–1406.
- [26] D. W. Urry, *Proc. Natl. Acad. Sci. USA* **1971**, *3*, 672–676.
- [27] G. N. Ramachandran, R. Chandrasekaran, *Indian J. Biochem. Biophys.* **1972**, *9*, 1–11.
- [28] L. Pauling, R. B. Corey, *Proc. Natl. Acad. Sci. USA* **1951**, *37*, 729–741.
- [29] P. DeSantis, S. Morosetti, R. Rizzo, *Macromolecules* **1974**, *7*, 52–58.
- [30] B. V. V. Prasad, R. Chandrasekaran, *Int. J. Pept. Protein Res.* **1977**, *10*, 129–138.
- [31] R. D. Hotchkiss, R. J. Dubos, *J. Biol. Chem.* **1941**, *141*, 171.
- [32] S.-I. Ishi, B. Witkop, *J. Am. Chem. Soc.* **1963**, *85*, 1832–1834.
- [33] R. L. M. Synge, *Biochem. J.* **1945**, *39*, 355.
- [34] R. Sarges, B. Witkop, *J. Am. Chem. Soc.* **1964**, *86*, 1861–1862.
- [35] R. Sarges, B. Witkop, *J. Am. Chem. Soc.* **1964**, *86*, 1862–1863.
- [36] S. B. Hladky, D. A. Haydon, *Nature* **1970**, *225*, 451–453.
- [37] M. C. Goodall, *Biochim. Biophys. Acta* **1970**, *219*, 471–478.
- [38] G. Spach, F. Heitz, *C. R. Acad. Sci. Ser. 3* **1973**, *276*, 1313–1375.
- [39] F. Ascoli, G. DeAngelis, F. DelBianco, P. DeSantis, *Biopolymers* **1975**, *14*, 1109–1114.
- [40] F. Heitz, B. Lotz, G. Spach, *J. Mol. Biol.* **1975**, *92*, 1–13.
- [41] B. Lotz, F. Colonna-Cesari, F. Heitz, G. Spach, *J. Mol. Biol.* **1976**, *106*, 915–942.
- [42] B. DiBlasio, M. Saviano, R. Fattorusso, A. Lombardi, C. Pedone, V. Valle, G. P. Lorenzi, *Biopolymers* **1994**, *34*, 1463–1468.
- [43] E. Benedetti, B. DiBlasio, C. Pedone, G. P. Lorenzi, L. Tomasic, V. Gramlich, *Nature* **1979**, *282*, 630.
- [44] B. DiBlasio, E. Benedetti, V. Pavone, C. Pedone, O. Spiniello, G. P. Lorenzi, *Biopolymers* **1989**, *28*, 193–201.
- [45] G. P. Lorenzi, L. Tomasic, H. Jäckle, *Makromol. Chem. Rapid Commun.* **1980**, *1*, 729–732.
- [46] G. P. Lorenzi, H. Jäckle, L. Tomasic, V. Rizzo, C. Pedone, *J. Am. Chem. Soc.* **1982**, *104*, 1728–1733.
- [47] G. P. Lorenzi, H. Jäckle, L. Tomasic, C. Pedone, *Biopolymers* **1983**, *22*, 157–161.
- [48] G. P. Lorenzi, L. Tomasic, *Makromol. Chem.* **1988**, *189*, 207–219.
- [49] G. P. Lorenzi, L. Tomasic, F. Bangerter, P. Neuenschwander, B. DiBlasio, *Helv. Chim. Acta* **1983**, *66*, 2129–2135.
- [50] G. P. Lorenzi, H. Jäckle, L. Tomasic, C. Pedone, B. DiBlasio, *Helv. Chim. Acta* **1983**, *66*, 158–167.
- [51] G. P. Lorenzi, V. Muri-Valle, F. Bangerter, *Helv. Chim. Acta* **1984**, *67*, 1588–1593.
- [52] G. P. Lorenzi, C. Gerber, H. Jäckle, *Biopolymers* **1984**, 1905–1916.
- [53] D. S. Kemp, B. R. Bowen, C. C. Muendel, *J. Org. Chem.* **1990**, *55*, 4650–4657.
- [54] J. S. Nowick, S. Insaf, *J. Am. Chem. Soc.* **1997**, *119*, 10903–10908.
- [55] T. D. Clark, J. M. Buriak, K. Kobayashi, M. P. Isler, D. E. McRee, M. R. Ghadiri, *J. Am. Chem. Soc.* **1998**, *120*, 8949–8962.
- [56] G. P. Lorenzi, C. Gerber, H. Jäckle, *Macromolecules* **1985**, *18*, 154–159.
- [57] E. F. Schoch, D. U. Römer, G. P. Lorenzi, *Int. J. Pept. Protein Res.* **1994**, *44*, 10–18.
- [58] R. Chandrasekaran, B. V. V. Prasad, *Crit. Rev. Biochem.* **1978**, *5*, 188–191.
- [59] B. A. Wallace, K. Ravikumar, *Jerusalem Symp. Quantum Chem. Biochem.* **1988**, *21*, 103–113.
- [60] B. A. Wallace, K. Ravikumar, *Science* **1988**, *241*, 182–187.
- [61] B. A. Wallace, *Prog. Biophys. Mol. Biol.* **1992**, *57*, 59–69.
- [62] D. A. Langs, *Science* **1988**, *241*, 188–191.
- [63] D. A. Langs, *Biopolymers* **1989**, *28*, 259–266.
- [64] D. A. Langs, G. D. Smith, C. Courseille, G. Precigoux, M. Hospital, *Proc. Natl. Acad. Sci. USA* **1991**, *88*, 5345–5349.
- [65] D. A. Doyle, B. A. Wallace, *Biochem. Soc. Trans.* **1994**, *22*, 1043–1045.
- [66] D. A. Doyle, B. A. Wallace, *J. Mol. Biol.* **1997**, *266*, 963–977.
- [67] O. S. Andersen, J. T. Durkin, R. E. Koeppe II, *Jerusalem Symp. Quantum Chem. Biochem.* **1988**, *21*, 115–132.
- [68] J. D. Lear, Z. R. Wasserman, W. F. DeGrado, *Science* **1988**, *240*, 1177–1181.
- [69] J. C. Nelson, J. G. Saven, J. S. Moore, P. G. Wolynes, *Science* **1997**, *277*, 1793–1796.
- [70] J. S. Moore, *Acc. Chem. Res.* **1997**, *30*, 402–413.
- [71] S. H. Gellman, *Acc. Chem. Res.* **1998**, *31*, 173–180.
- [72] D. H. Appella, L. A. Christianson, D. A. Klein, D. R. Powell, X. Huang, J. J. Barchi, Jr., S. H. Gellman, *Nature* **1997**, *387*, 381–384.
- [73] D. H. Appella, L. A. Christianson, I. L. Karle, D. R. Powell, S. H. Gellman, *J. Am. Chem. Soc.* **1996**, *118*, 13071–13072.
- [74] R. B. Prince, S. A. Barnes, J. S. Moore, *J. Am. Chem. Soc.* **2000**, *122*, 2758–2762.
- [75] R. B. Prince, L. Brunsveld, E. W. Meijer, J. S. Moore, *Angew. Chem.* **2000**, *112*, 234–236; *Angew. Chem. Int. Ed.* **2000**, *39*, 228–230.
- [76] M. S. Gin, T. Yokozawa, R. B. Prince, J. S. Moore, *J. Am. Chem. Soc.* **1999**, *121*, 2643–2644.
- [77] R. B. Prince, T. Okada, J. S. Moore, *Angew. Chem.* **1999**, *111*, 245–249; *Angew. Chem. Int. Ed.* **1999**, *38*, 233–236.
- [78] J. C. Nelson, J. K. Young, J. S. Moore, *J. Org. Chem.* **1996**, *61*, 8160–8168.
- [79] J. D. Hartgerink, M. R. Ghadiri, *Proc. 2nd OUMS (Osuka, Japan)* **1996**, pp. 181–188.
- [80] J. D. Hartgerink, T. D. Clark, M. R. Ghadiri, *Chem. Eur. J.* **1998**, *4*, 1367–1372.
- [81] J. M. Buriak, M. R. Ghadiri, *Mater. Sci. Eng. C* **1997**, *4*, 207–212.
- [82] R. Ghadiri, *Adv. Mater.* **1995**, *7*, 675–677.
- [83] L. Tomasic, G. P. Lorenzi, *Helv. Chim. Acta* **1987**, *70*, 1012–1016.
- [84] V. Pavone, E. Benedetti, B. D. Blasio, A. Lombardi, C. Pedone, G. P. Lorenzi, *Biopolymers* **1989**, *28*, 215–223.

- [85] M. R. Ghadiri, J. R. Granja, R. A. Milligan, D. E. McRee, N. Khazanovich, *Nature* **1993**, 366, 324–327.
- [86] M. E. Polaskova, N. J. Ede, J. N. Lambert, *Aust. J. Chem.* **1998**, 51, 535–540.
- [87] N. Khazanovich, J. R. Granja, D. E. McRee, R. A. Milligan, M. R. Ghadiri, *J. Am. Chem. Soc.* **1994**, 116, 6011–6012.
- [88] J. D. Hartgerink, J. R. Granja, R. A. Milligan, M. R. Ghadiri, *J. Am. Chem. Soc.* **1996**, 118, 43–50.
- [89] A. Karlström, A. Udén, *Biopolymers* **1997**, 41, 1–4.
- [90] M. R. Ghadiri, J. R. Granja, L. K. Buehler, *Nature* **1994**, 369, 301–304.
- [91] H. S. Kim, L. K. Buehler, J. R. Granja, M. R. Ghadiri, unpublished results.
- [92] H. S. Kim, J. D. Hartgerink, M. R. Ghadiri, *J. Am. Chem. Soc.* **1998**, 120, 4417–4424.
- [93] J. R. Granja, M. R. Ghadiri, *J. Am. Chem. Soc.* **1994**, 116, 10785–10786.
- [94] M. Engels, D. Bashford, M. R. Ghadiri, *J. Am. Chem. Soc.* **1995**, 117, 9151–9158.
- [95] O. S. Smart, J. Breed, G. R. Smith, M. S. P. Sansom, *Biophys. J.* **1997**, 72, 1109–1126.
- [96] M. Saviano, A. Lombardi, C. Pedone, B. Diblasio, X. C. Sun, G. P. Lorenzi, *J. Inclusion Phenom.* **1994**, 18, 27–36.
- [97] X. C. Sun, G. P. Lorenzi, *Helv. Chim. Acta* **1994**, 77, 1520–1526.
- [98] M. R. Ghadiri, K. Kobayashi, J. R. Granja, R. K. Chadha, D. E. McRee, *Angew. Chem.* **1995**, 107, 76–78; *Angew. Chem. Int. Ed. Engl.* **1995**, 34, 93–95.
- [99] K. Kobayashi, J. R. Granja, M. R. Ghadiri, *Angew. Chem.* **1995**, 107, 79–81; *Angew. Chem. Int. Ed. Engl.* **1995**, 34, 95–98.
- [100] K.-C. Chou, M. Pottle, G. Nemethy, Y. Ueda, H. A. Scheraga, *J. Mol. Biol.* **1982**, 162, 89–112.
- [101] C. Gailer, M. Feigel, *J. Comput. Aided Mol. Des.* **1997**, 11, 273–277.
- [102] T. D. Clark, M. R. Ghadiri, *J. Am. Chem. Soc.* **1995**, 117, 12364–12365.
- [103] T. D. Clark, M. R. Ghadiri, *Chem. Eur. J.* **1999**, 5, 782–792.
- [104] C. H. Hassall, *Proc. Am. Pept. Symp.* **1972**, 3, 153–157.
- [105] I. L. Karle, B. K. Handa, C. H. Hassall, *Acta Crystallogr. Sect. B* **1975**, 31, 555–560.
- [106] D. Seebach, J. L. Matthews, A. Meden, T. Wessels, C. Baerlocher, L. B. McCusker, *Helv. Chim. Acta* **1997**, 80, 173–182.
- [107] T. D. Clark, L. K. Buehler, M. R. Ghadiri, *J. Am. Chem. Soc.* **1998**, 120, 651–656.
- [108] D. Ranganathan, V. Haridas, C. S. Sundari, D. Balasubramanian, K. P. Madhusudan, R. Roy, I. L. Karle, *J. Org. Chem.* **1999**, 64, 9230–9240.
- [109] D. Ranganathan, C. Lakshmi, I. L. Karle, *J. Am. Chem. Soc.* **1999**, 121, 6103–6107.
- [110] D. Ranganathan, V. Haridas, R. Gilardi, I. L. Karle, *J. Am. Chem. Soc.* **1998**, 120, 10793–10800.
- [111] G. W. Coates, A. R. Dunn, L. M. Henling, D. A. Dougherty, R. H. Grubbs, *Angew. Chem.* **1997**, 109, 290–293; *Angew. Chem. Int. Ed. Engl.* **1997**, 36, 248–251.
- [112] G. W. Coates, A. R. Dunn, L. M. Henling, J. W. Ziller, E. B. Lobkovsky, R. H. Grubbs, *J. Am. Chem. Soc.* **1998**, 120, 3641–3649.
- [113] M. Weck, A. R. Dunn, K. Matsumoto, G. W. Coates, E. B. Lobkovsky, R. H. Grubbs, *Angew. Chem.* **1999**, 111, 2909–2912; *Angew. Chem. Int. Ed.* **1999**, 38, 2741–2745.
- [114] S. M. Ngola, D. A. Dougherty, *J. Org. Chem.* **1998**, 63, 4566–4567.
- [115] J. C. Ma, D. A. Dougherty, *Chem. Rev.* **1997**, 97, 1303–1324.
- [116] S. Mecozzi, A. P. West, Jr., D. A. Dougherty, *Proc. Natl. Acad. Sci. USA* **1996**, 93, 10566–10571.
- [117] D. A. Dougherty, *Science* **1996**, 271, 163–168.
- [118] R. A. Kumpf, D. A. Dougherty, *Science* **1993**, 261, 1708–1710.
- [119] A. Harada, J. Li, M. Kamachi, *Nature* **1992**, 356, 325–327.
- [120] A. Harada, J. Li, M. Kamachi, *Nature* **1993**, 364, 516–518.
- [121] G. Li, L. B. McGown, *Science* **1994**, 264, 249–251.
- [122] G. Pistolis, A. Malliaris, *J. Phys. Chem.* **1996**, 100, 15562–15568.
- [123] G. Pistolis, A. Malliaris, *J. Phys. Chem. B* **1998**, 102, 1095–1101.
- [124] R. C. Teitelbaum, S. L. Ruby, T. J. Marks, *J. Am. Chem. Soc.* **1978**, 100, 3215–3217.
- [125] W. Hinrichs, G. Buettner, M. Steifa, C. Betzel, V. Zabel, B. Pfanemuehler, W. Saenger, *Science* **1987**, 238, 205–208.
- [126] P. R. Ashton, C. L. Brown, S. Menzer, S. A. Nepogodiev, J. F. Stoddart, D. J. Williams, *Chem. Eur. J.* **1996**, 2, 580–591.
- [127] P. R. Ashton, S. J. Cantrill, G. Gattuso, S. Menzer, S. A. Nepogodiev, A. N. Shipway, J. F. Stoddart, D. J. Williams, *Chem. Eur. J.* **1997**, 3, 1299–1314.
- [128] G. Gattuso, S. Menzert, S. A. Nepogodiev, J. F. Stoddart, D. J. Williams, *Angew. Chem.* **1997**, 109, 1615–1617; *Angew. Chem. Int. Ed. Engl.* **1997**, 36, 1451–1454.
- [129] J. Zhang, J. S. Moore, *J. Am. Chem. Soc.* **1994**, 116, 2655–2656.
- [130] A. S. Shetty, J. Zhang, J. S. Moore, *J. Am. Chem. Soc.* **1996**, 118, 1019–1027.
- [131] J. Zhang, J. S. Moore, *J. Am. Chem. Soc.* **1992**, 114, 9701–9702.
- [132] D. Venkataraman, S. Lee, J. Zhang, J. S. Moore, *Nature* **1994**, 371, 591–593.
- [133] J.-M. Lehn, J. Mathête, A.-M. Levelut, *J. Chem. Soc. Chem. Commun.* **1985**, 1794–1796.
- [134] J. Malthête, A.-M. Levelut, J.-M. Lehn, *J. Chem. Soc. Chem. Commun.* **1992**, 1434–1436.
- [135] L. Isaacs, D. N. Chin, N. Bowden, Y. Xia, G. M. Whitesides, *Perspect. Supramol. Chem.* **1999**, 4, 1–46.
- [136] J. P. Mathias, C. T. Seto, E. E. Simanek, G. M. Whitesides, *J. Am. Chem. Soc.* **1994**, 116, 1725–1736.
- [137] J. P. Mathias, E. E. Simanek, G. M. Whitesides, *J. Am. Chem. Soc.* **1994**, 116, 4326–4340.
- [138] J. P. Mathias, E. E. Simanek, J. A. Zerkowski, C. T. Seto, G. M. Whitesides, *J. Am. Chem. Soc.* **1994**, 116, 4316–4325.
- [139] I. S. Choi, X. Li, E. E. Simanek, R. Akaba, G. M. Whitesides, *Chem. Mater.* **1999**, 11, 684–690.
- [140] G. Cevc, D. Marsh, *Phospholipid Bilayers: Physical Principles and Models*, Wiley, New York, **1987**.
- [141] J. N. Israelachvili, S. Marcelja, R. G. Horn, *Q. Rev. Biophys.* **1980**, 13, 121–200.
- [142] R. B. Gennis, *Biomembranes: Molecular Structure and Function*, Springer, New York, **1989**.
- [143] J. N. Israelachvili, D. J. Mitchell, B. W. Ninham, *J. Chem. Soc. Faraday Trans. 2* **1976**, 72, 1525–1568.
- [144] H. Hauser, I. Pascher, S. Sundell, *J. Mol. Biol.* **1980**, 137, 249–264.
- [145] M. W. Tate, S. M. Gruner, *Biochemistry* **1989**, 28, 4245–4253.
- [146] J. M. Seddon, *Biochim. Biophys. Acta* **1990**, 1031, 1–69.
- [147] D. F. O'Brien, B. Armitage, A. Benedicto, D. E. Bennett, H. G. Lamparski, Y.-S. Lee, W. Srisiri, T. M. Sisson, *Acc. Chem. Res.* **1998**, 31, 861–868.
- [148] W. Srisiri, T. M. Sisson, D. F. O'Brien, K. M. McGrath, Y. Han, S. M. Gruner, *J. Am. Chem. Soc.* **1997**, 119, 4866–4873.
- [149] V. Percec, J. Heck, D. Tomazos, F. Falkenberg, H. Blackwell, G. Ungar, *J. Chem. Soc. Perkin Trans. 1* **1993**, 2799–2811.
- [150] V. Percec, D. Tomazos, J. Heck, H. Blackwell, G. Ungar, *J. Chem. Soc. Perkin Trans. 2* **1994**, 31–44.
- [151] V. Percec, G. Johansson, G. Ungar, J. Zhou, *J. Am. Chem. Soc.* **1996**, 118, 9855–9866.
- [152] V. Percec, C.-H. Ahn, T. K. Bera, G. Ungar, D. J. P. Yearley, *Chem. Eur. J.* **1999**, 5, 1070–1083.
- [153] V. Percec, J. A. Heck, D. Tomazos, G. Ungar, *J. Chem. Soc. Perkin Trans. 2* **1993**, 2381–2388.
- [154] S. Stewart, G. Liu, *Angew. Chem.* **2000**, 112, 348–352; *Angew. Chem. Int. Ed.* **2000**, 39, 340–344.
- [155] N. Nakashima, S. Asakuma, J. M. Kim, T. Kunitake, *Chem. Lett.* **1984**, 1709–1712.
- [156] J. H. Fuhrhop, P. Schnieder, J. Rosenberg, E. Boekema, *J. Am. Chem. Soc.* **1987**, 109, 3387–3390.
- [157] K. Yamada, H. Ihara, T. Ide, T. Fukumoto, C. Hirayama, *Chem. Lett.* **1984**, 1713–1716.
- [158] D. D. Archibald, P. Yager, *Biochemistry* **1992**, 31, 9045–9055.
- [159] P. Yager, P. E. Schoen, *Mol. Cryst. Liq. Cryst.* **1984**, 106, 371–81.
- [160] P. Yager, P. E. Schoen, C. Davies, R. Price, A. Singh, *Biophys. J.* **1985**, 48, 899–906.
- [161] B. R. Ratna, S. Baral-Tosh, B. Kahn, J. M. Schnur, A. S. Rudolph, *Chem. Phys. Lipids* **1992**, 63, 47–53.
- [162] J. H. Georger, A. Singh, R. R. Price, J. M. Schnur, P. Yager, P. E. Schoen, *J. Am. Chem. Soc.* **1987**, 109, 6169–6175.
- [163] B. N. Thomas, C. R. Safinya, R. J. Plano, N. A. Clark, *Science* **1995**, 267, 1635–1638.

- [164] W. Helfrich, J. Prost, *Phys. Rev. A* **1988**, *38*, 3065–3068.
- [165] J. V. Selinger, F. C. MacKintosh, J. M. Schnur, *Phys. Rev. E* **1996**, *53*, 3804–3818.
- [166] J. M. Schnur, B. R. Ratna, J. V. Selinger, A. Singh, G. Jyothi, K. R. K. Easwaran, *Science* **1994**, *264*, 945–947.
- [167] M. S. Spector, K. R. K. Easwaran, G. Jyothi, J. V. Selinger, A. Singh, J. M. Schnur, *Proc. Natl. Acad. Sci. USA* **1996**, *93*, 12943–12946.
- [168] J. M. Schnur, P. E. Schoen, P. Yager, J. M. Calvert, J. H. Georger, R. Price, US 4911981, **1990**.
- [169] B. A. Cornell, V. L. Braach-Maksyutis, L. King, P. D. Osman, B. Raguse, L. Wiczorek, R. J. Pace, *Nature* **1997**, *387*, 580–583.
- [170] D. U. Roemer, G. P. Lorenzi, A. L. Weisenhorn, *Thin Solid Films* **1994**, *238*, 285–289.
- [171] A. L. Weisenhorn, D. U. Roemer, G. P. Lorenzi, *Langmuir* **1992**, *8*, 3145–3149.
- [172] K. Motesharei, M. R. Ghadiri, *J. Am. Chem. Soc.* **1998**, *120*, 1347.
- [173] K. Motesharei, M. R. Ghadiri, *J. Am. Chem. Soc.* **1997**, *119*, 11306–11312.
- [174] O. Braha, B. Walker, S. Cheley, J. J. Kasianowicz, L. Song, J. E. Gouaux, H. Bayley, *Chem. Biol.* **1997**, *4*, 497–505.
- [175] L.-Q. Gu, O. Braha, S. Conlan, S. Cheley, H. Bayley, *Nature* **1999**, *398*, 686–690.
- [176] J. Sanchez-Quesada, H. Bayley, M. R. Ghadiri, O. Braha, *J. Am. Chem. Soc.* **2000**, *122*, 11757–11766.
- [177] S. Fernandez-Lopez, M. S. Kim, E. C. Choi, M. Delgado, J. R. Granja, A. Khasanov, K. Kraehenbuehl, G. Long, D. A. Weinberger, K. Wilcoxen, M. R. Ghadiri, unpublished results.
- [178] K. Fukasaku, K. Takeda, K. Shiraishi, *J. Phys. Soc. Jpn.* **1997**, *66*, 3387–3390.
- [179] H. Okamoto, M. Kasahara, K. Takeda, K. Shiraishi, *Pept. Sci.* **1999**, *36*, 67–70.
- [180] P. Carloni, W. Andreoni, M. Parrinello, *Phys. Rev. Lett.* **1997**, *79*, 761–764.
- [181] J. P. Lewis, N. H. Pawley, O. F. Sankey, *J. Phys. Chem. B* **1997**, *101*, 10576–10583.
- [182] R. A. Jishi, N. C. Braier, C. T. White, J. W. Mintmire, *Phys. Rev. B* **1998**, *58*, 16009–16011.
- [183] V. Barachevsky, *Proc. SPIE Int. Soc. Opt. Eng.* **1997**, *3055*, 2–11.
- [184] V. Barachevsky, M. Alimov, V. Nazarov, *Proc. SPIE Int. Soc. Opt. Eng.* **1998**, *3468*, 293–301.
- [185] V. A. Barachevsky, *Proc. SPIE Int. Soc. Opt. Eng.* **1997**, *2968*, 77–86.
- [186] C. B. McArdle, *Appl. Photochromic Polym. Syst.* **1992**, 1–30.
- [187] Z. Sekkat, W. Knoll, *Adv. Photochem.* **1997**, *22*, 117–195.
- [188] J. A. Delaire, K. Nakatani, *Chem. Rev.* **2000**, *100*, 1817–1845.
- [189] I. Willner, *Acc. Chem. Res.* **1997**, *30*, 347–356.
- [190] I. Y. Galaev, B. Mattiasson, *Trends Biotechnol.* **1999**, *17*, 335–340.
- [191] M.-H. Hao, H. A. Scheraga, *Acc. Chem. Res.* **1998**, *31*, 433–440.
- [192] M. R. Ghadiri, A. K. Fernholz, *J. Am. Chem. Soc.* **1990**, *112*, 9633–9635.
- [193] M. R. Ghadiri, C. Choi, *J. Am. Chem. Soc.* **1990**, *112*, 1630–1632.
- [194] M. S. Vollmer, T. D. Clark, C. Steinem, M. R. Ghadiri, *Angew. Chem.* **1999**, *111*, 1703–1706; *Angew. Chem. Int. Ed.* **1999**, *38*, 1598–1601.
- [195] C. Steinem, A. Janshoff, M. S. Vollmer, M. R. Ghadiri, *Langmuir* **1999**, *15*, 3956–3964.
- [196] H. Rapaport, H. S. Kim, K. Kjaer, P. B. Howes, S. Cohen, J. Als-Nielsen, M. R. Ghadiri, L. Leiserowitz, M. Lahav, *J. Am. Chem. Soc.* **1999**, *121*, 1186–1191.
- [197] J. D. Hartgerink, M. R. Ghadiri, unpublished results.
- [198] D. D. Archibald, S. Mann, *Nature* **1993**, *364*, 430–433.
- [199] R. C. Smith, W. M. Fischer, D. L. Gin, *J. Am. Chem. Soc.* **1997**, *119*, 4092–4093.
- [200] L. Smilowitz, A. Hays, A. J. Heeger, G. Wang, J. E. Bowers, *J. Chem. Phys.* **1993**, *98*, 6504–6509.
- [201] S. A. Jenekhe, J. A. Osaheni, *Chem. Mater.* **1994**, *6*, 1906–1909.
- [202] M. Kawa, J. M. J. Frechet, *Thin Solid Films* **1998**, *331*, 259–263.
- [203] M. Kawa, J. M. J. Frechet, *Chem. Mater.* **1998**, *10*, 286–296.
- [204] H. Deng, D. L. Gin, R. C. Smith, *J. Am. Chem. Soc.* **1998**, *120*, 3522–3523.
- [205] S. A. Miller, E. Kim, D. H. Gray, D. L. Gin, *Angew. Chem.* **1999**, *111*, 3206–3210; *Angew. Chem. Int. Ed.* **1999**, *38*, 3022–3026.
- [206] O. Bouloussa, J. Michel, M. Dupeyrat, *Stud. Phys. Theor. Chem.* **1983**, *24*, 87–95.
- [207] M. G. Khaledi, A. H. Rodgers, *Anal. Chim. Acta* **1990**, *239*, 121–128.
- [208] J. L. Smart, J. A. McCammon, *J. Am. Chem. Soc.* **1996**, *118*, 2283–2284.
- [209] D. W. Urry, *J. Phys. Chem. B* **1997**, *101*, 11007–11028.
- [210] G. Jones, *Org. React. N. Y.* **1967**, *15*, 204–299.
- [211] E. Kimura, H. Hashimoto, T. Koike, *J. Am. Chem. Soc.* **1996**, *118*, 10963–10970.
- [212] R. A. Thompson, S. Allenmark, *J. Colloid Interface Sci.* **1992**, *148*, 241–246.
- [213] S. Bhattacharya, K. Snehalatha, *Langmuir* **1995**, *11*, 4653–4660.
- [214] O. A. El Seoud, *Adv. Colloid Interface Sci.* **1989**, *30*, 1–30.
- [215] R. R. Price, M. Patchan, A. Clare, D. Rittschof, J. Bonaventura, *Biofouling* **1992**, *6*, 207–216.
- [216] R. Price, M. Patchan, *J. Microencapsulation* **1991**, *8*, 301–306.
- [217] R. R. Price, M. Patchan, *J. Microencapsulation* **1993**, *10*, 215–222.